DLR TAU Simulations for the Second AIAA Sonic Boom Prediction Workshop

Jochen Kirz

Ralf Rudnik

DLR

Outline

- Flow Solver and Computing platform

- Cases analyzed and Grids used
- Simulation Settings and Flow Solver Convergence

- Simulation Results
- Highlights

- Summary / Conclusions
- Questions / Discussion

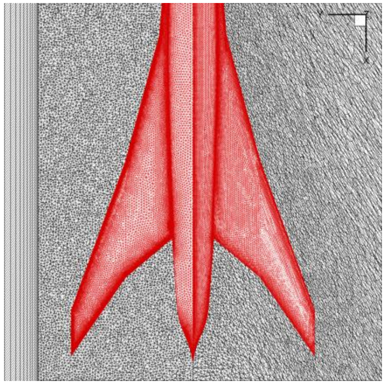

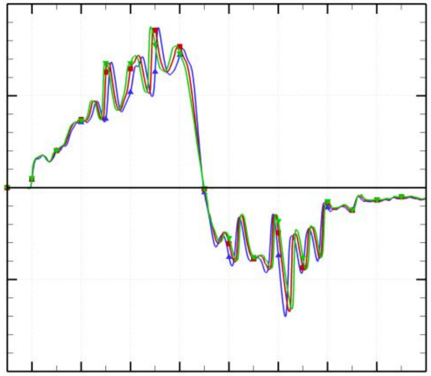

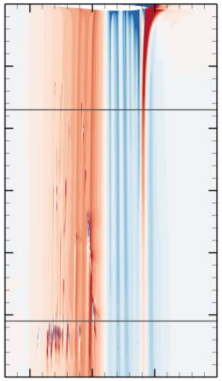

DLR

Flow Solver and Computing Platform

- DLR TAU Code
  - Unstructured finite-volume
  - Euler, RANS
  - Hybrid grids
  - Backward Euler and Runge-Kutta timestepping
  - Central and upwind schemes (Roe, Van Leer, AUSMDV, AUSMP(W+))
  - 2nd order upwind limiter functions (Barth Jesperson, Venkatakrishnan, SRR)

- $C^2A^2S^2E$-2 Cluster
  - parallel
  - distributed memory
  - 1 computing node (24 cores) per 300.000 grid nodes

Cases Analyzed and Grids Used

AXIE 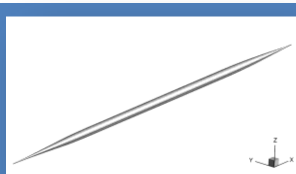	JWB 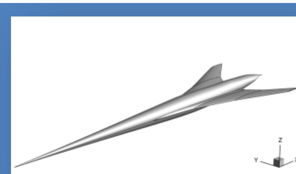	C25D flow through 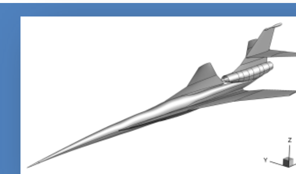	
axie-inv-mixed-256	jwb-invisc.C100	c25d-flo-inv-mixed-200	c25d-flo-visc-mixed-200
axie-inv-mixed-200	jwb-invisc.C080	c25d-flo-inv-mixed-160	c25d-flo-visc-mixed-160
axie-inv-mixed-160	jwb-invisc.C064	c25d-flo-inv-mixed-128	c25d-flo-visc-mixed-128
axie-inv-mixed-128		c25d-flo-inv-mixed-100	c25d-flo-visc-mixed-100
axie-inv-mixed-100		c25d-flo-inv-mixed-080	c25d-flo-visc-mixed-080
		c25d-flo-inv-mixed-064	c25d-flo-visc-mixed-064
axie-inv-tet-256	jwb-inv-tet-100	c25d-flo-inv-tet-200	c25d-flo-visc-tet-200
axie-inv-tet-200	jwb-inv-tet-083	c25d-flo-inv-tet-160	c25d-flo-visc-tet-160
axie-inv-tet-160	jwb-inv-tet-070	c25d-flo-inv-tet-128	c25d-flo-visc-tet-128
axie-inv-tet-128		c25d-flo-inv-tet-100	c25d-flo-visc-tet-100
axie-inv-tet-100		c25d-flo-inv-tet-080	c25d-flo-visc-tet-080
		c25d-flo-inv-tet-064	c25d-flo-visc-tet-064

black: workshop-provided grids blue: CENTAUR-generated grids

DLR

Cases Analyzed and Grids Used

CENTAUR-generated Grids for JWB case

- Hybrid Euler grids
  - Unaligned tetrahedrons in cylindrical inner part
  - Mach cone aligned hexahedrons in farfield

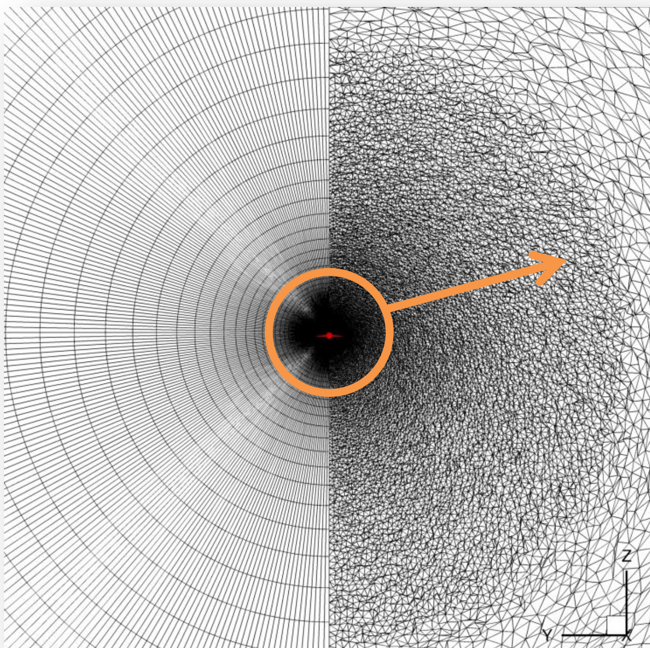

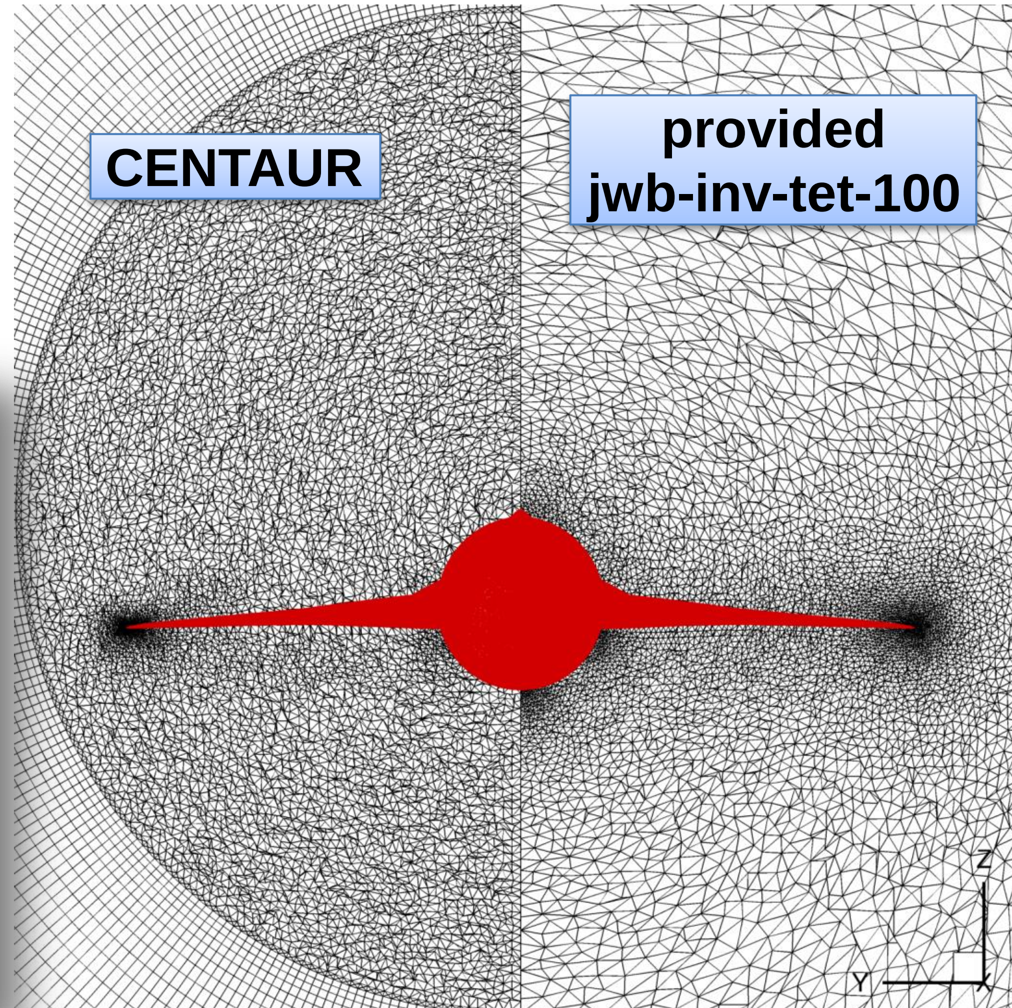

DLR

Cases Analyzed and Grids Used

CENTAUR-generated Grids for JWB case

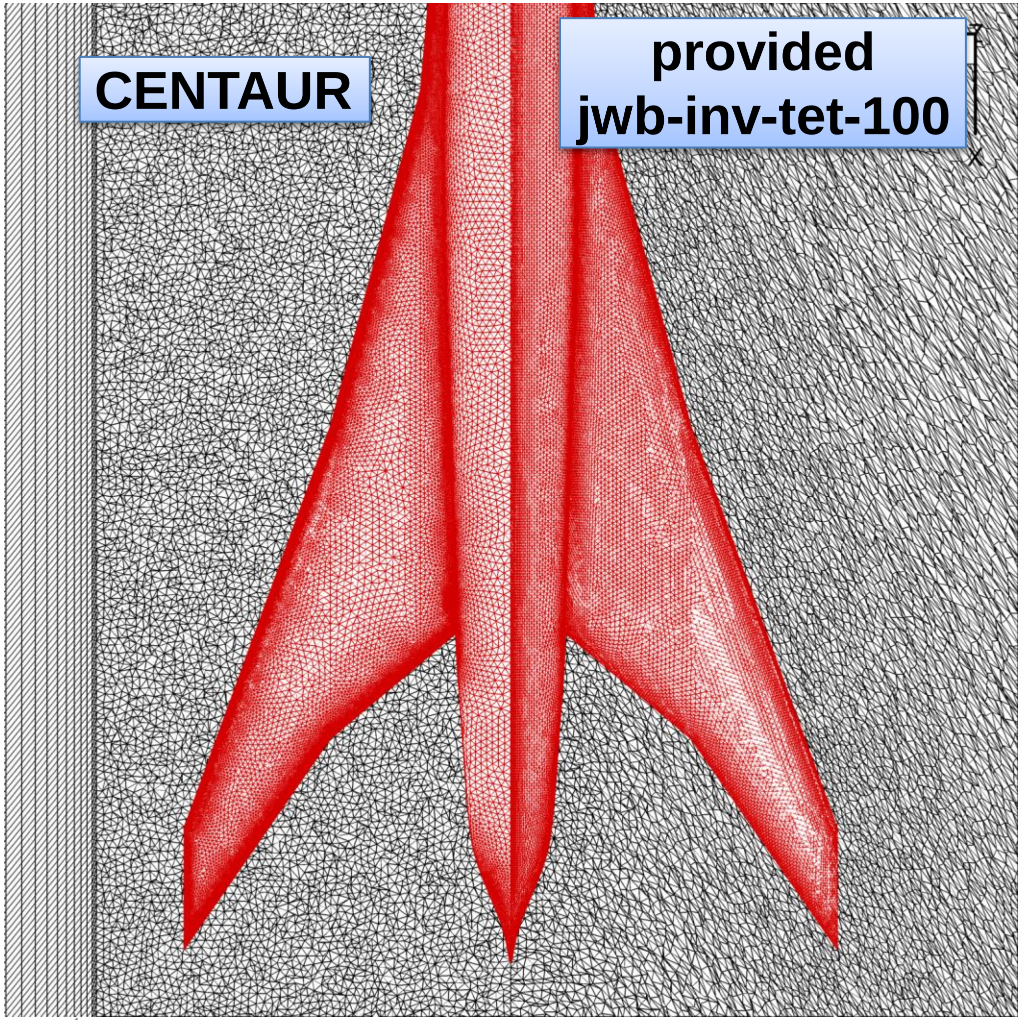

- Surface resolution (triangles) of coarse CENTAUR grid similar to coarse workshop-provided grid

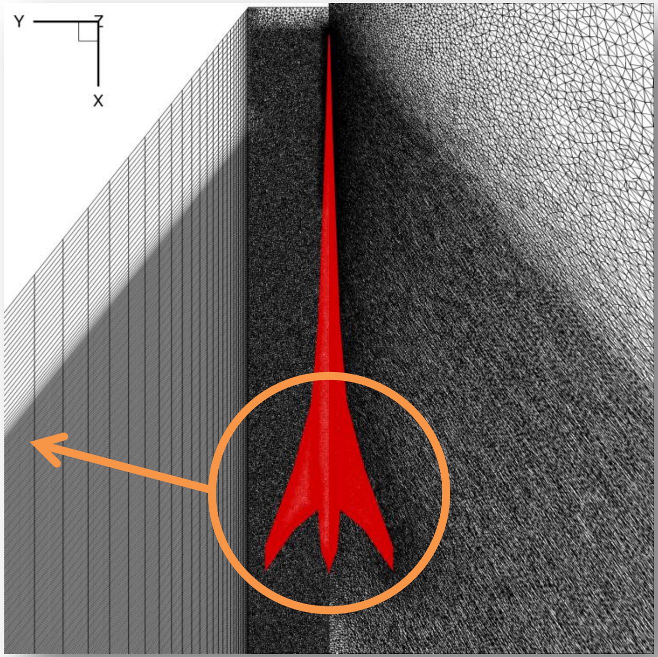

Cases Analyzed and Grids Used
CENTAUR-generated Grids

- Hybrid Euler grids
  - Unaligned tetrahedrons in cylindrical inner part
  - Mach cone aligned hexahedrons in farfield
- Surface resolution (triangles) of coarse CENTAUR grid similar to coarse workshop-provided grid
- Series of uniformly refined grids

Grid	Nodes	Hexahedrons	Tetrahedrons
jwb-invisc.C100	8,122,061	4,268,264	20,694,950
jwb-invisc.C080	15,110,113	8,412,624	36,385,888
jwb-invisc.C064	29,292,032	16,877,552	68,351,196
jwb-inv-tet-100	6,491,425	-	37,397,159

Simulation Settings and Flow Solver Convergence
Typical Convergence History (jwb-inv-tet-070)

- Euler / SA in negative formulation for viscous calculations
- LUSGS
- AUSMDV 2nd order
- Venkatakrishnan limiter
- Green Gauss reconstruction of gradients

- Mach and CFL ramping
- Convergence criteria 15000 Iterations

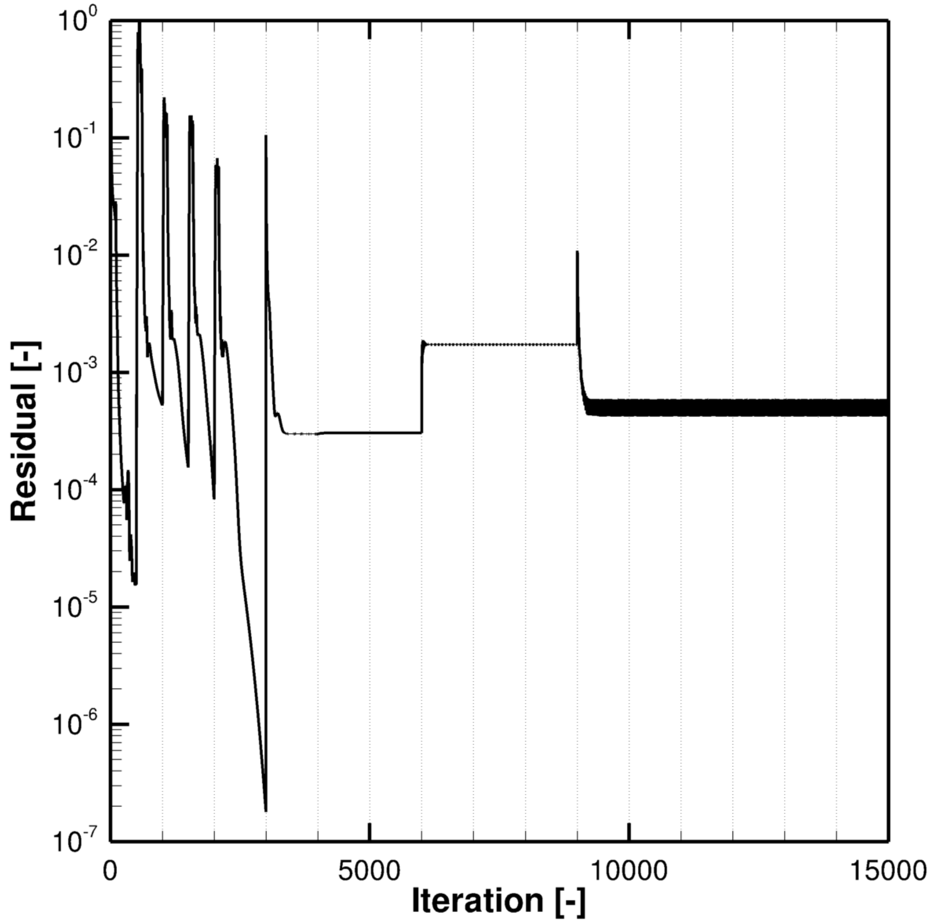

Simulation Settings and Flow Solver Convergence

Typical Convergence History (jwb-inv-tet-070)

- Euler / SA in negative formulation for viscous calculations
- LUSGS
- AUSMDV 2nd order
- Venkatakrishnan limiter
- Green Gauss reconstruction of gradients

- Mach and CFL ramping
- Convergence criteria 15000 Iterations

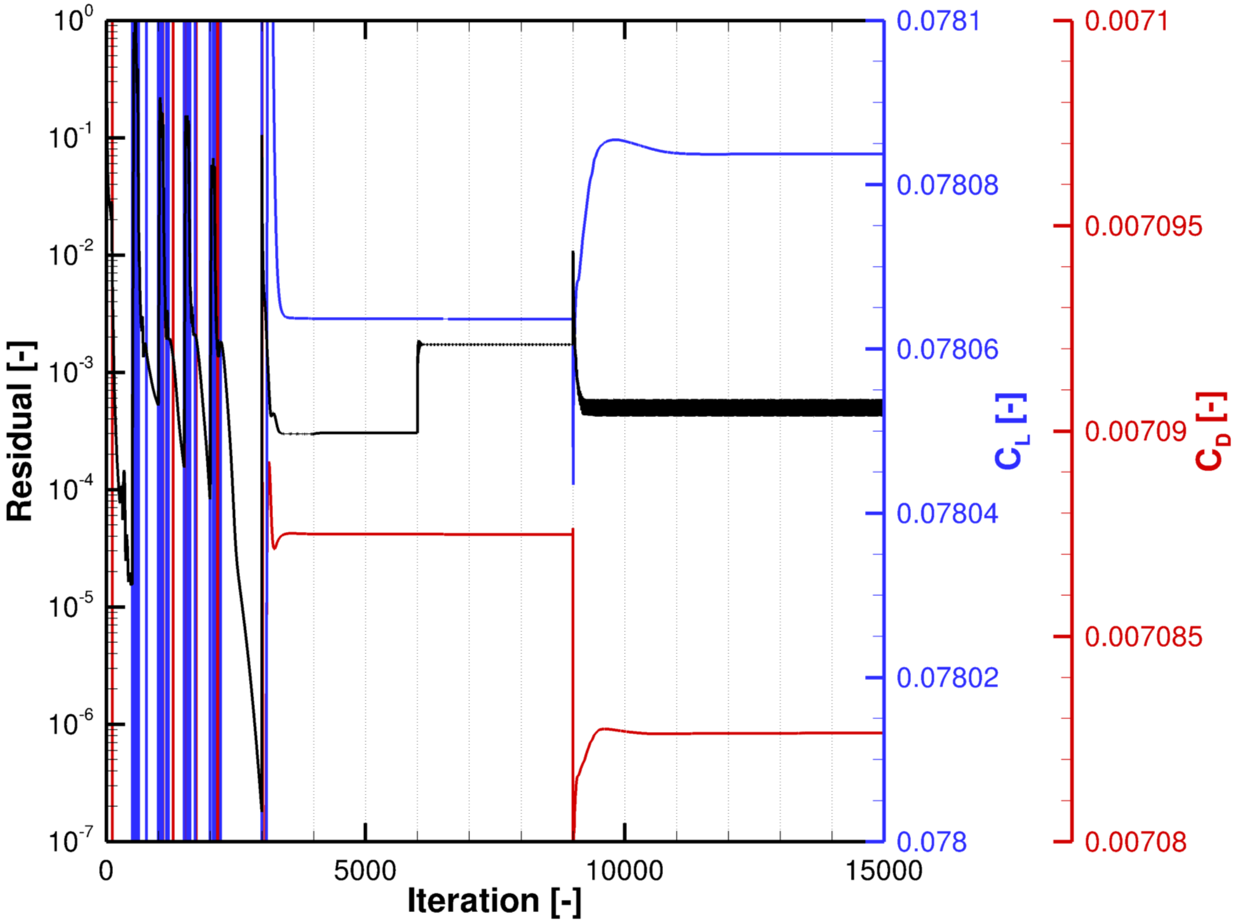

Outline

- Flow Solver and Computing platform
- Cases analyzed and Grids used
- Simulation Settings and Flow Solver Convergence
- Simulation Results
- Highlights
- Summary / Conclusions
- Questions / Discussion

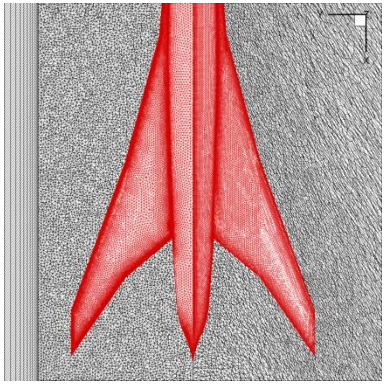

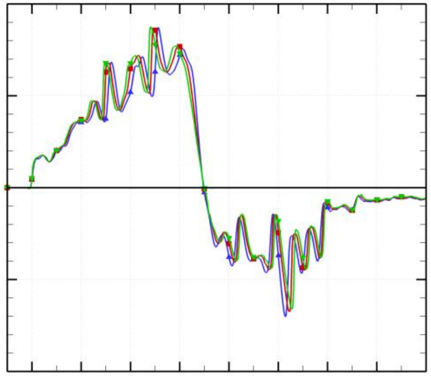

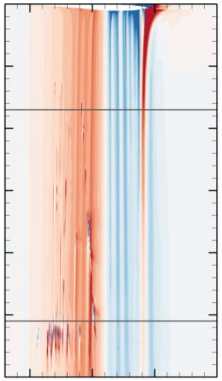

DLR

Results AXIE

Pressure Contours and near field signatures

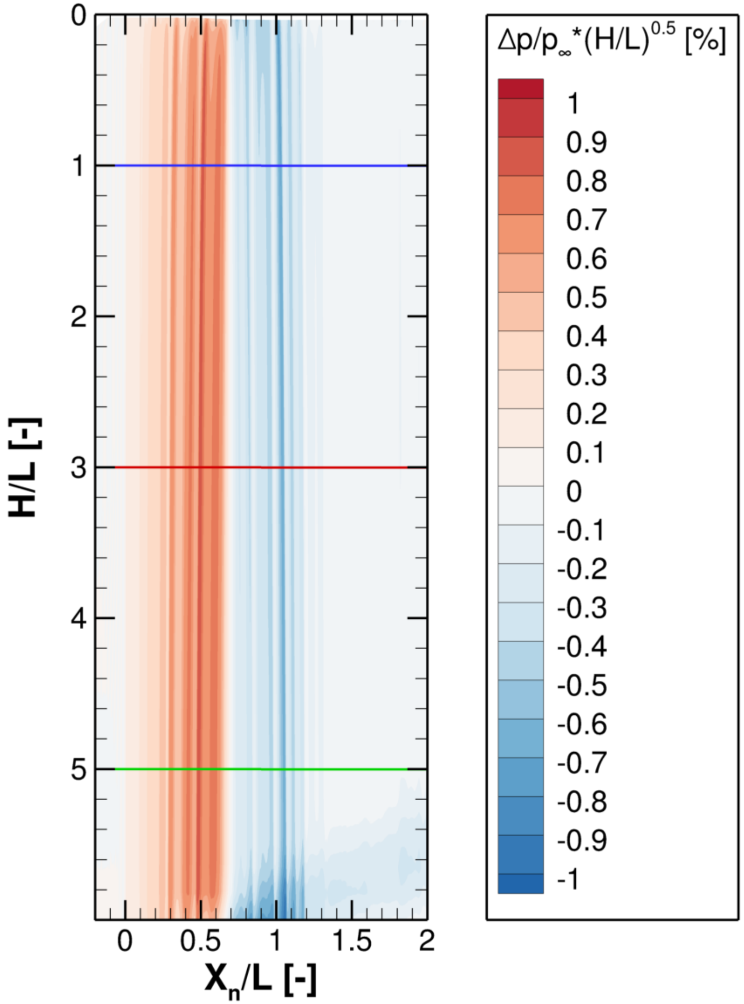

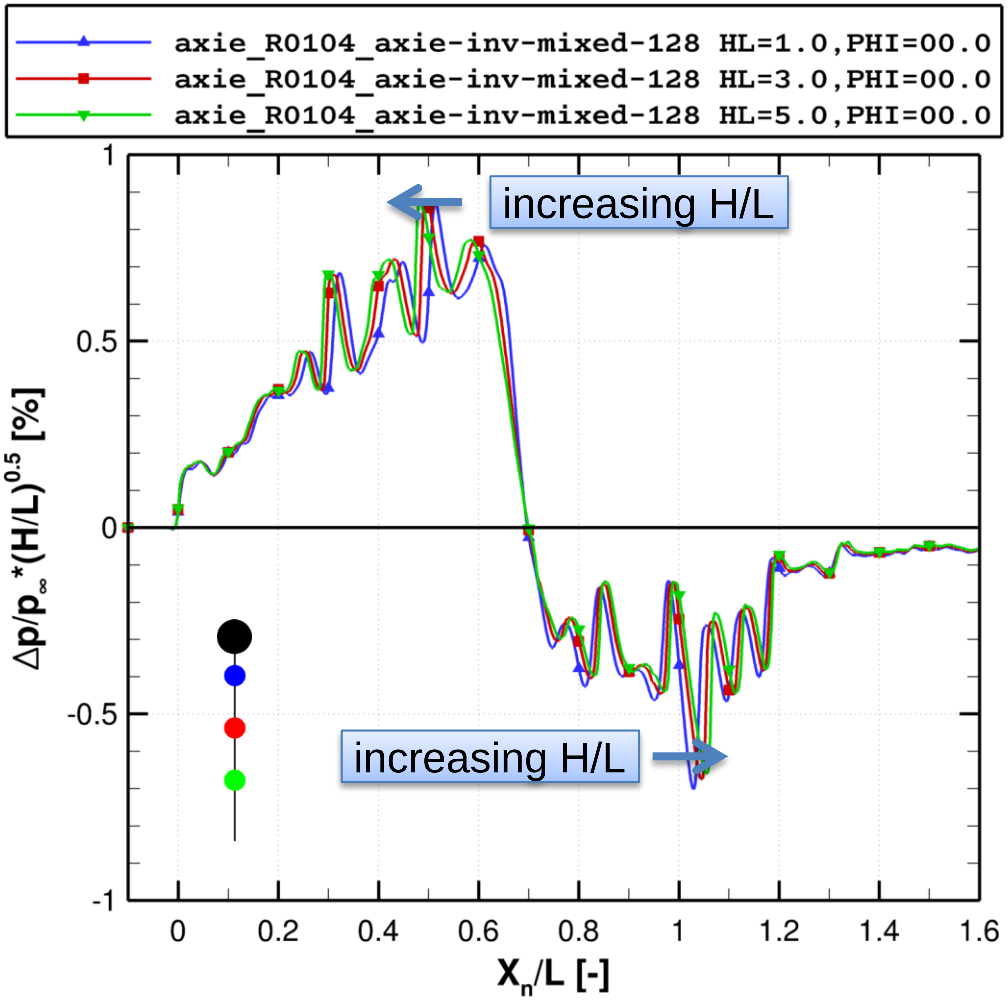

Results AXIE
Signature Convergence

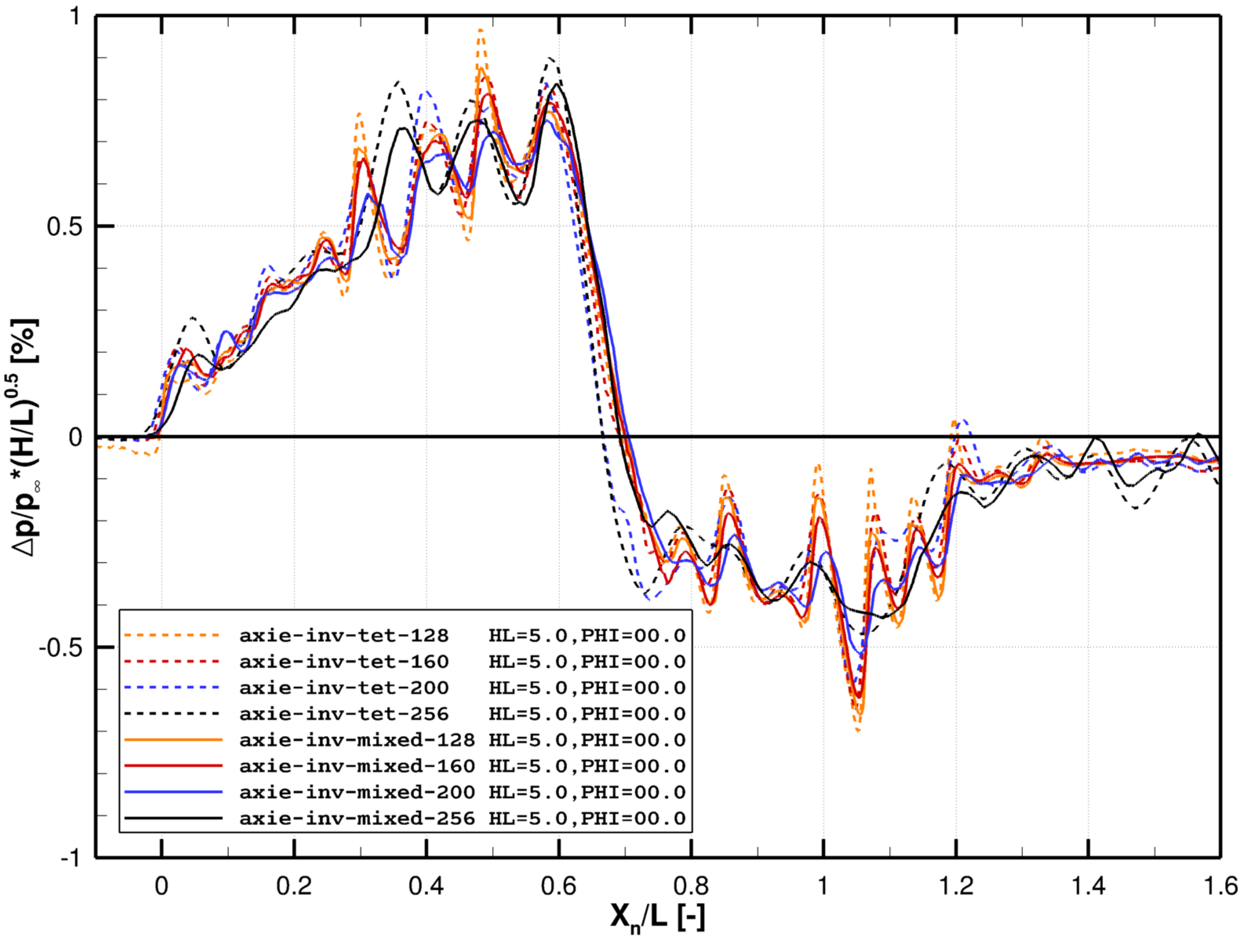

- No obvious convergence with grid resolution
- Positions of the shocks and expansions are similar for the medium to fine grids, but vary for the coarsest grids
- Tetrahedral grids result in higher peak pressures

Results JWB

Pressure Contours and near field signatures

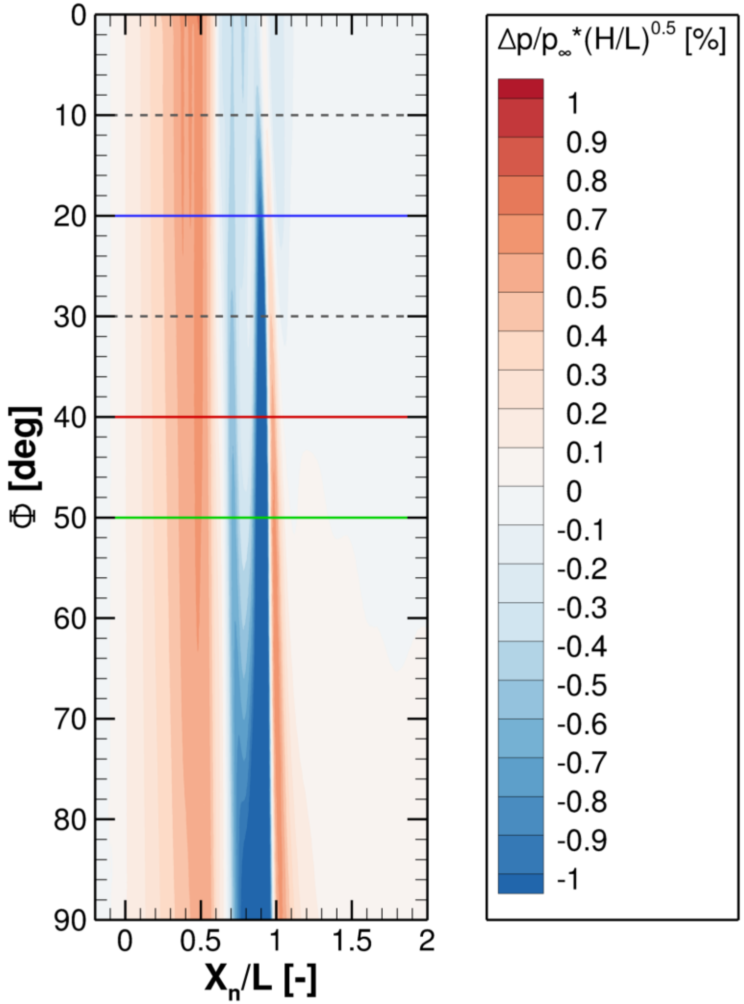

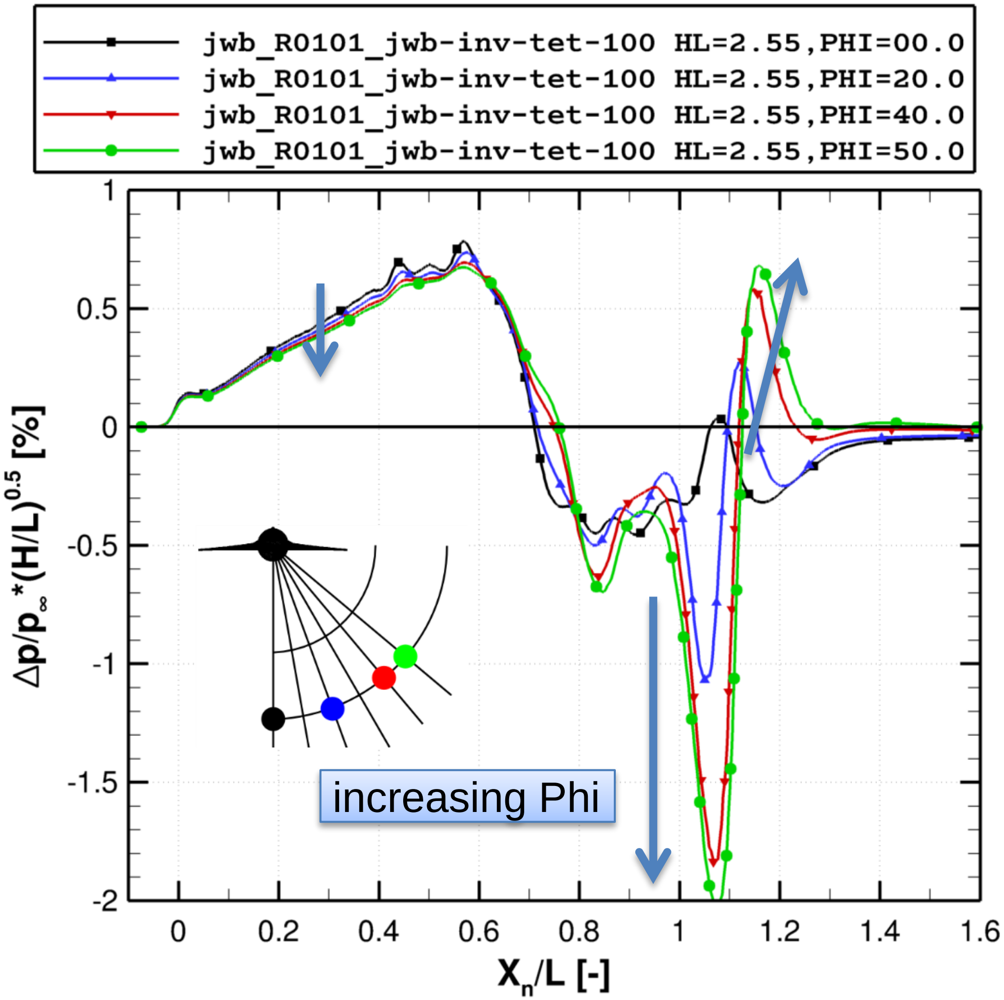

Results JWB
Signature Convergence

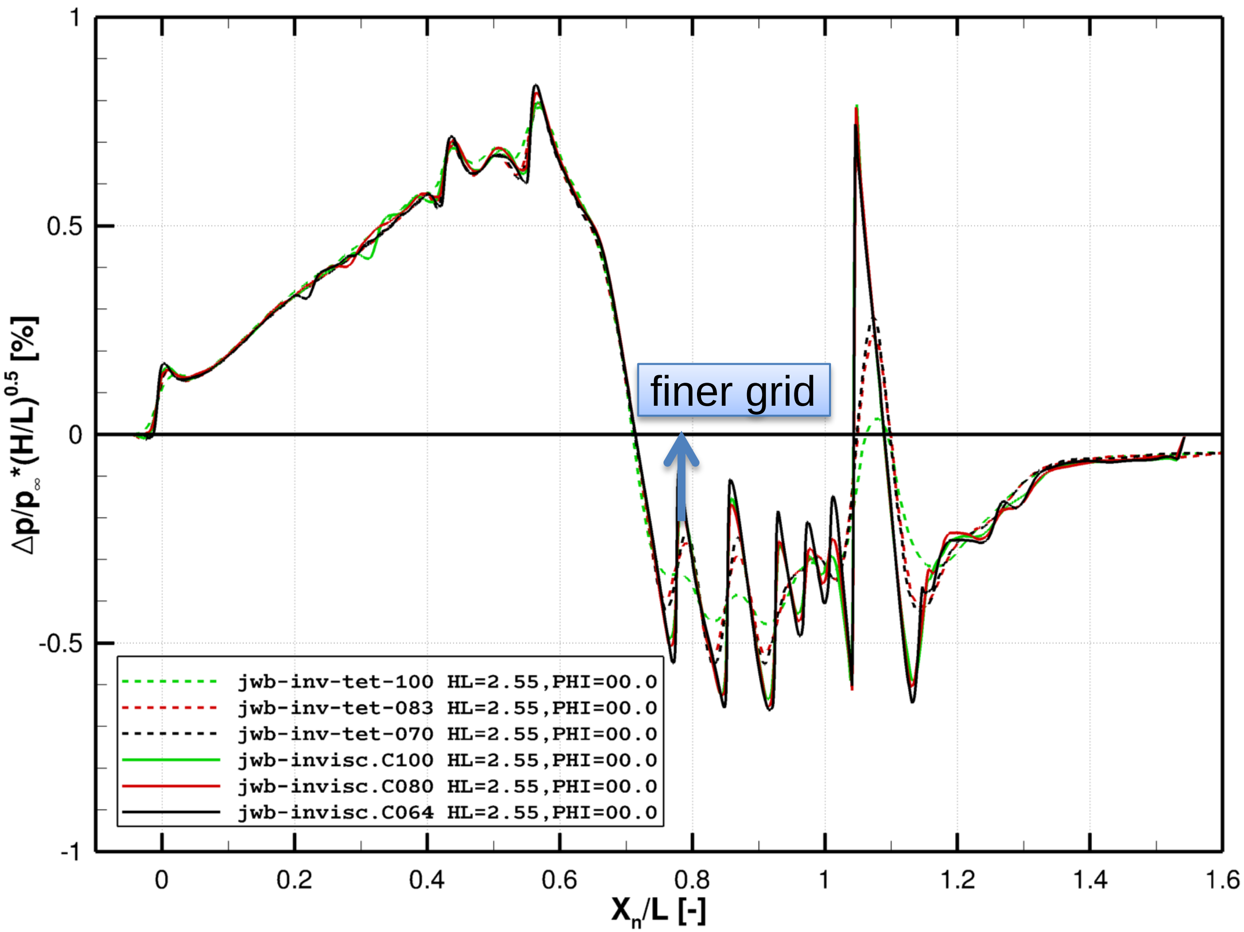

- Smooth pressure rise for the provided grids
- Slight expansions at the pressure rise for the generated grids
- Positions of shocks and expansions agree for all grids
- CENTAUR grids lead to higher peak pressures, especially in the aft part of the signature

Results C25D flow-through

Pressure Contours and near field signatures

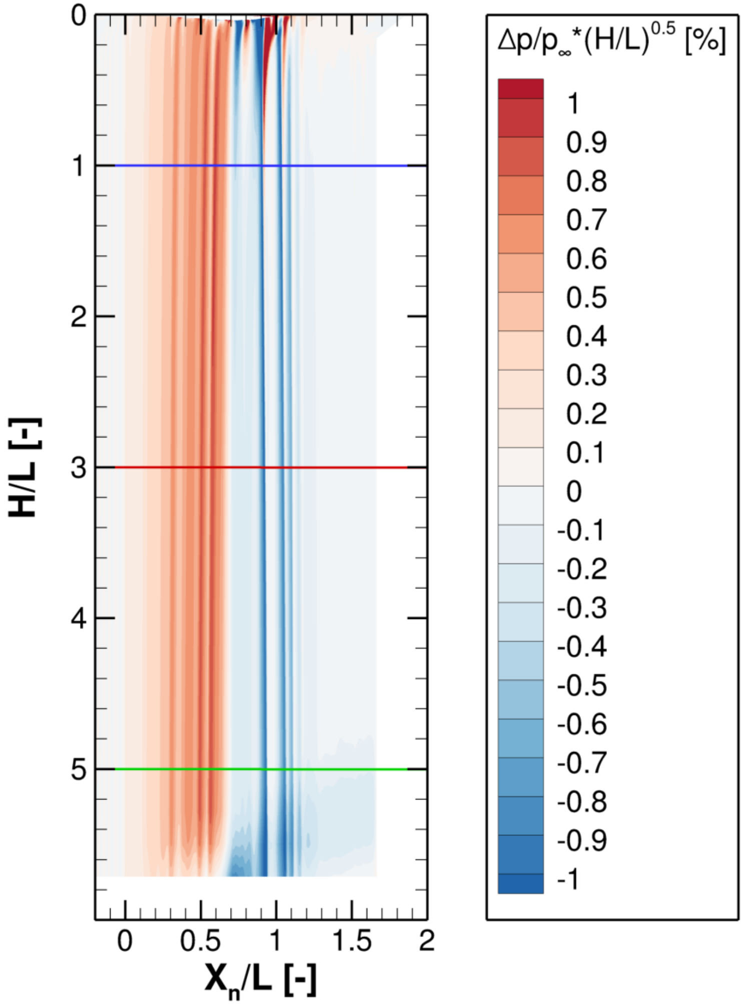

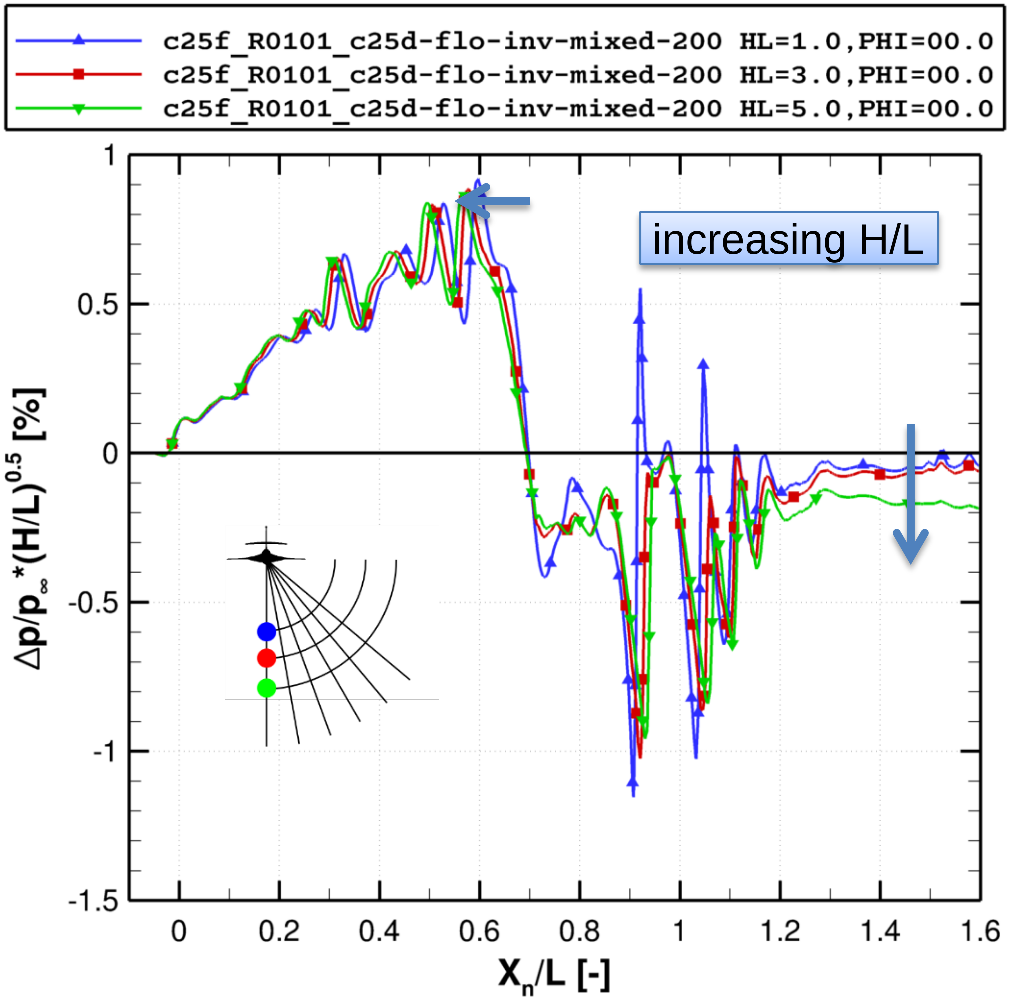

Results C25D flow-through

Signature Convergence

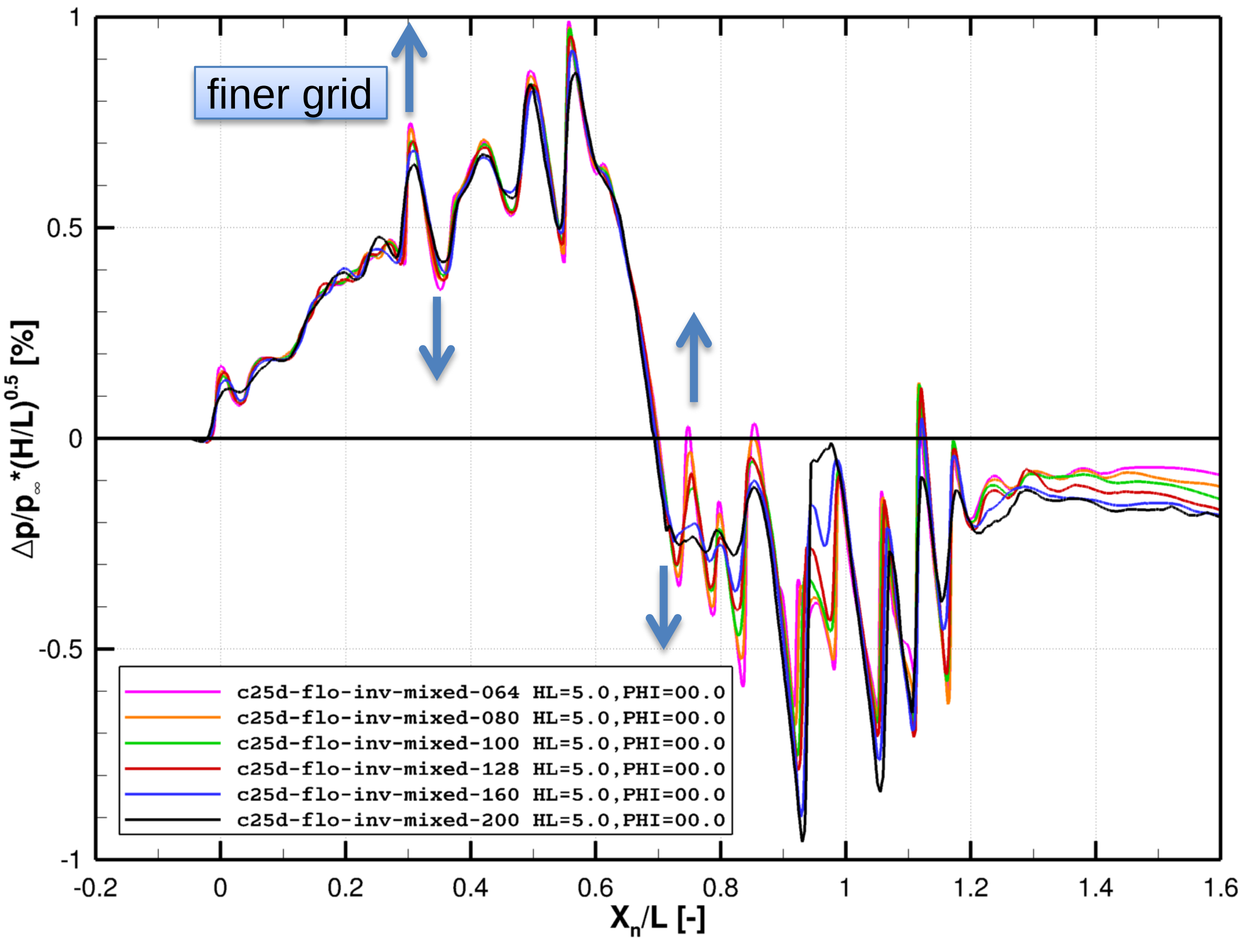

- Fine grids lead to stronger shocks and expansions than coarse grids

Results C25D flow-through

Viscous in comparison to inviscid calculations

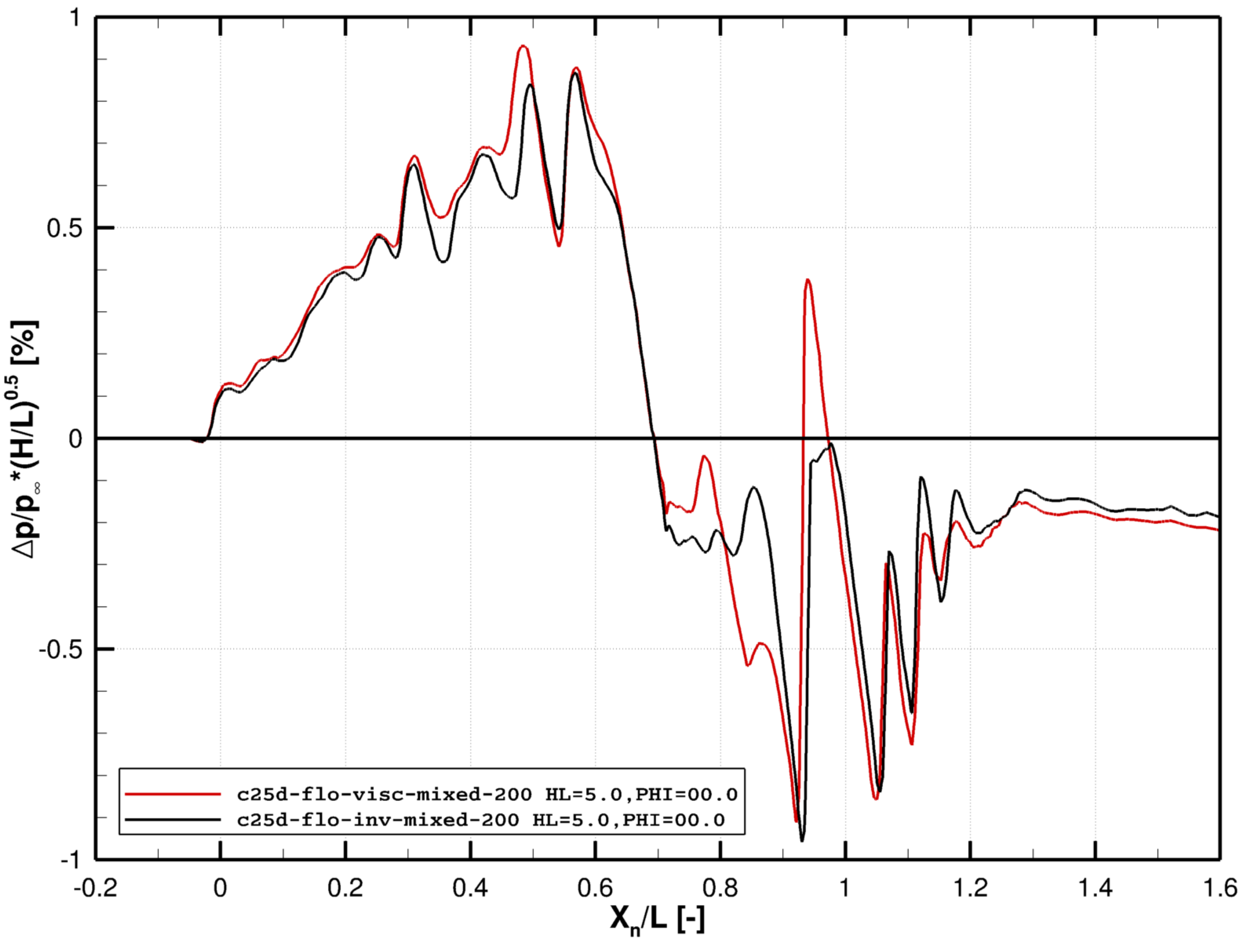

- Fine grids lead to stronger shocks and expansions than coarse grids
- Influence of viscosity stronger than influence of grid resolution

Highlights

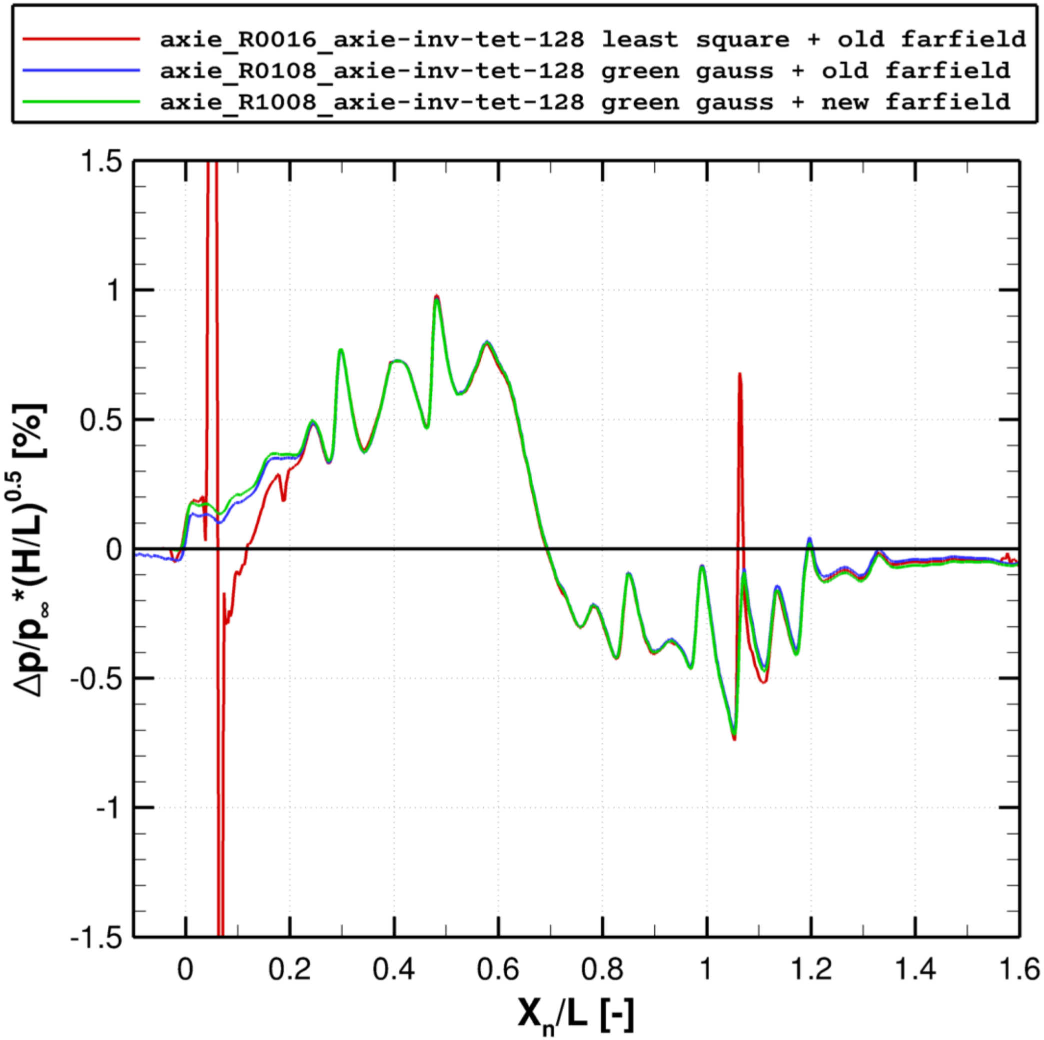

- Unphysical pressures for fine tetrahedrons with large aspect ratio in combination with least square reconstruction of gradients (red line)
- Unphysical pressures for large H/L at inflow, outflow and farfield boundary conditions (blue line)

Highlights

Unphysical pressures for fine tetrahedrons with large aspect ratio in combination with least square reconstruction of gradients

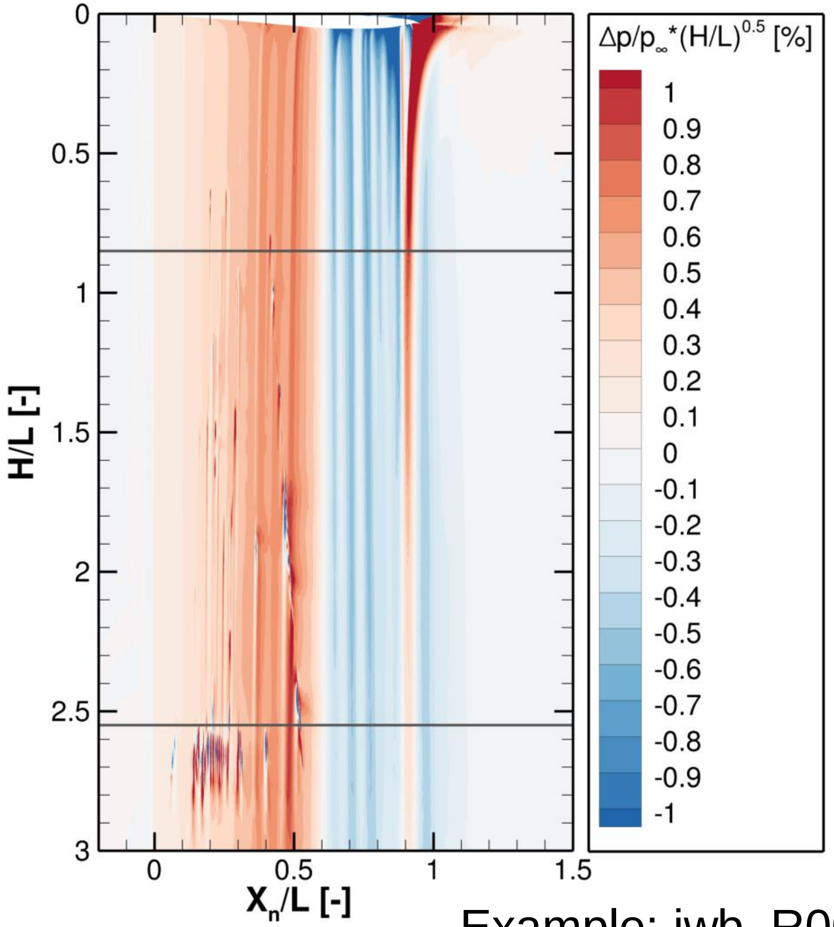

- Only appearing on purely tetrahedral grids
- Most significant on fine grids
- Independent of chosen upwind scheme and limiter

Example: jwb_R0003_jwb-inv-tet-070 (least square)

Highlights

Unphysical pressures for fine tetrahedrons with large aspect ratio in combination with least square reconstruction of gradients

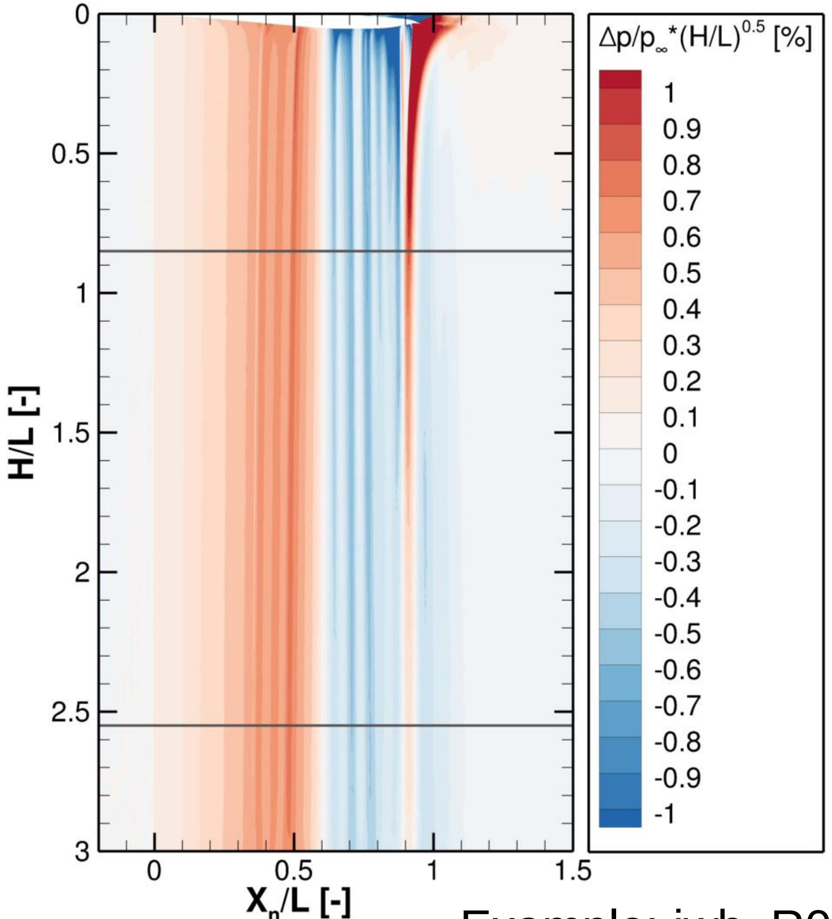

- Only appearing on purely tetrahedral grids
- Most significant on fine grids
- Independent of chosen upwind scheme and limiter

→ Resolved before submission by switching to Green Gauss reconstruction of gradients

Example: jwb_R0103_jwb-inv-tet-070 (Green Gauss)

Highlights

Unphysical pressures for large H/L at inflow, outflow and farfield boundary conditions

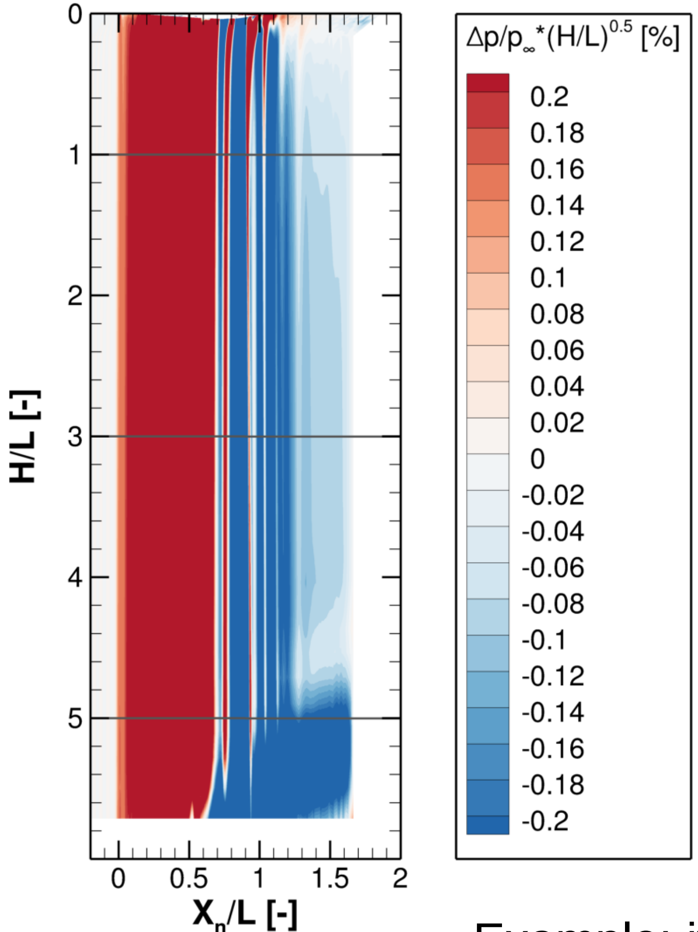

- The strength of the error follows clear patterns:
  - purely tetrahedral > mixed-element
  - viscous > inviscid
  - coarse > fine
  - for off-track angles up to 50 degrees the effect is lower but still existent

Example: jwb_R0026_c25d-flo-visc-tet-200 (old FF)

Highlights

Unphysical pressures for large H/L at inflow, outflow and farfield boundary conditions

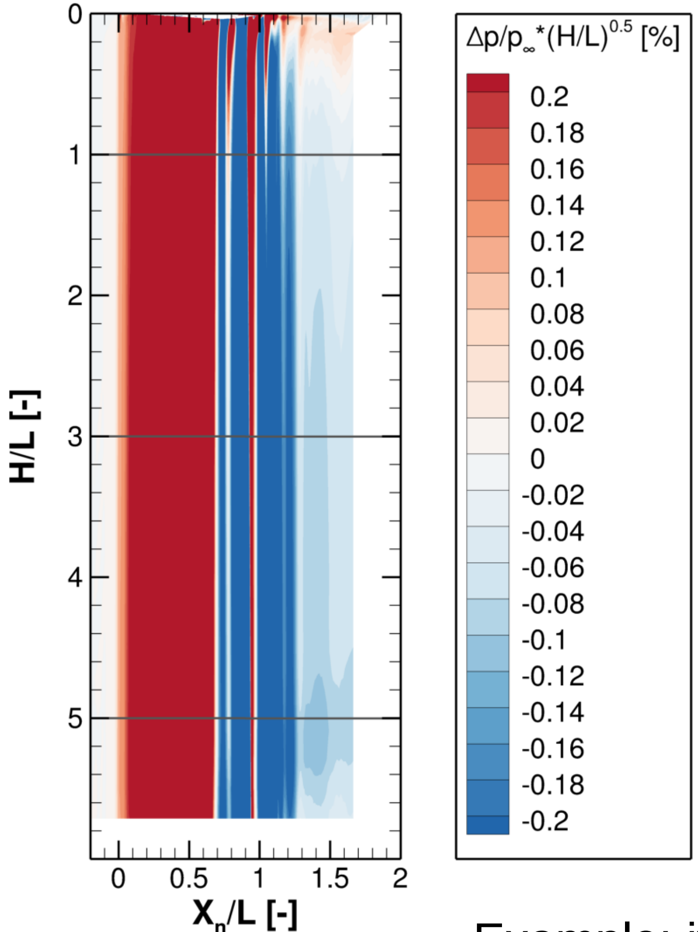

- The strength of the error follows clear patterns:
  - purely tetrahedral > mixed-element
  - viscous > inviscid
  - coarse > fine
  - for off-track angles up to 50 degrees the effect is lower but still existent

→Contacted by the committee

→Solution improved by changing the inflow, outflow and farfield boundary conditions, not completely resolved

→Work-around by increasing the farfield radius

Example: jwb_R1026_c25d-flo-visc-tet-200 (new FF)

Summary and Conclusions

- Positions of shocks and expansions
  - Similar for grids with medium to fine resolution
  - Different for very coarse grids
- Strength of shocks and expansions
  - Higher for fine grids compared to coarse grids
  - Higher for purely tetrahedral grids compared to mixed-element grids

- Influence of grid setup (tet/mixed) stronger than influence of grid resolution
- Influence of viscosity stronger than influence of grid setup
- Strong influence of numerical settings especially for tetrahedral farfields

→ The prediction of near-field pressure signatures with the DLR TAU Code is possible

→ Understanding of the origin of numerical errors in the farfield can be improved further

Questions/Discussion

DLR

Backup Slides

Normalization

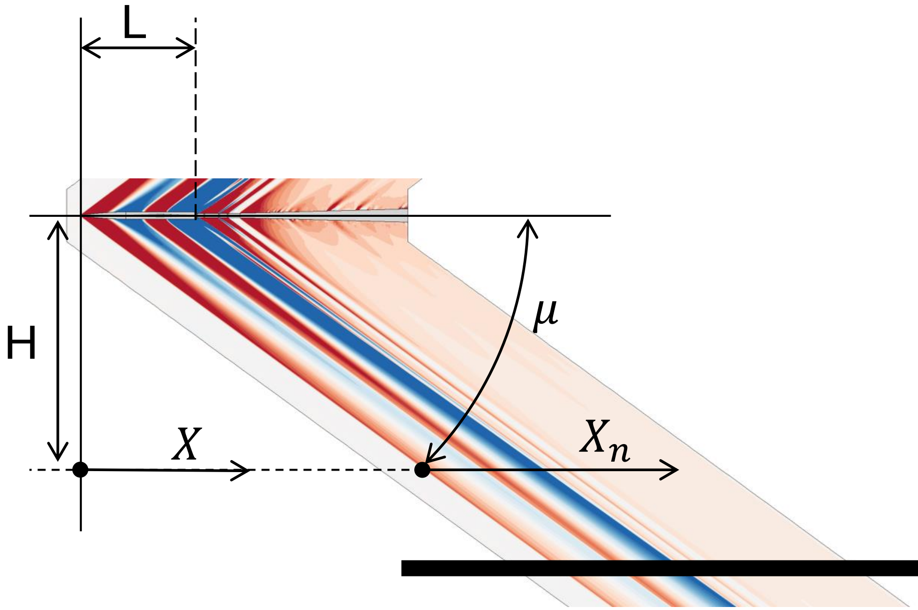

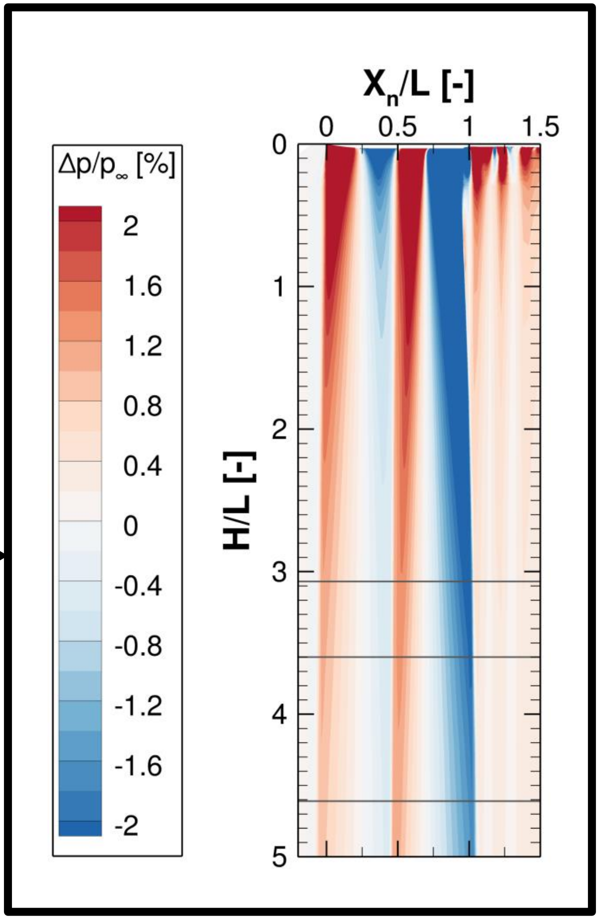

- Mach angle μ:

$$X_n = X - \frac{H}{\tan(\mu)}$$

- Body length L:
  → H/L
  → X_n/L

Results AXIE

Signatures H/L=1 (new FF)

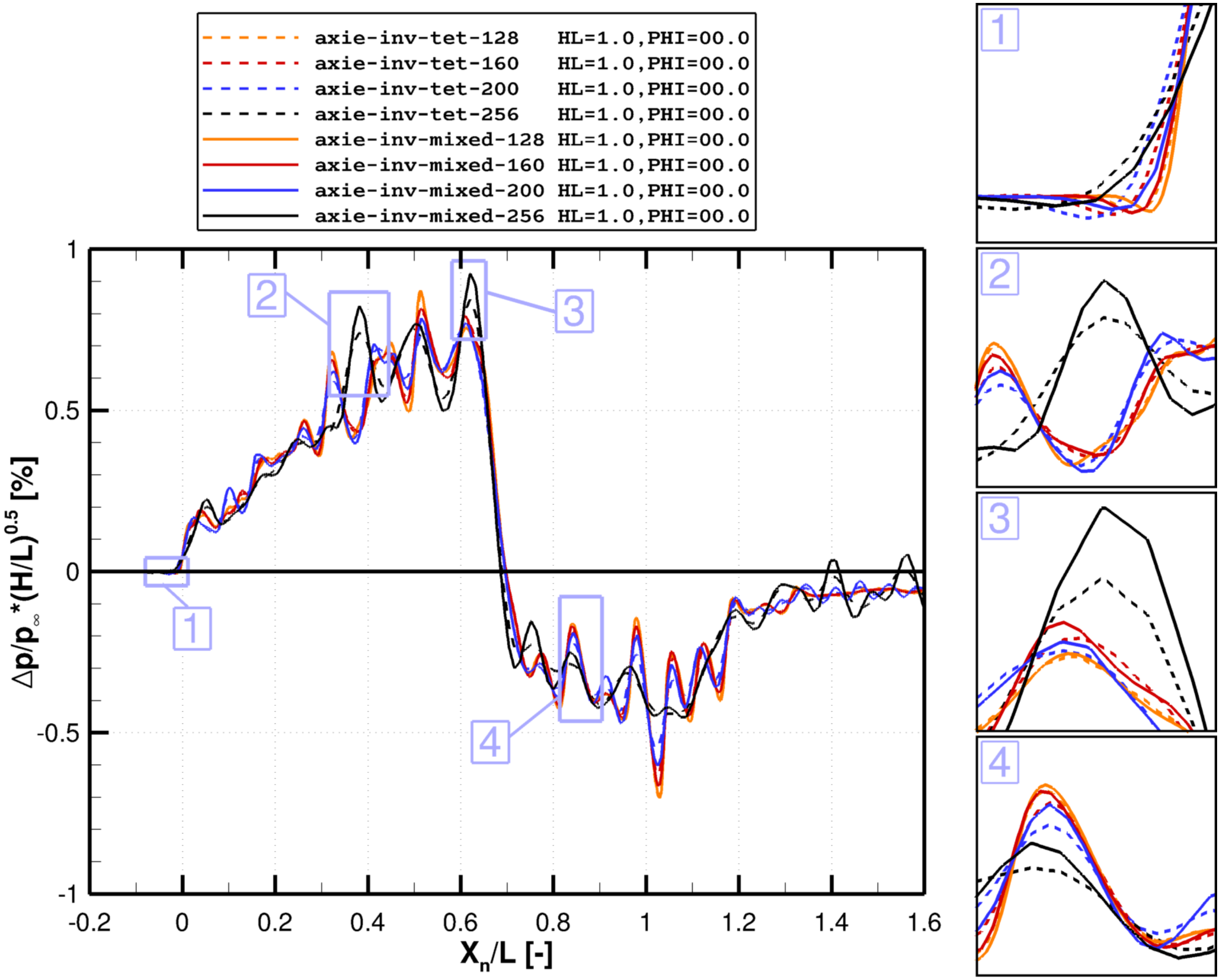

Results AXIE
Signatures H/L=3 (new FF)

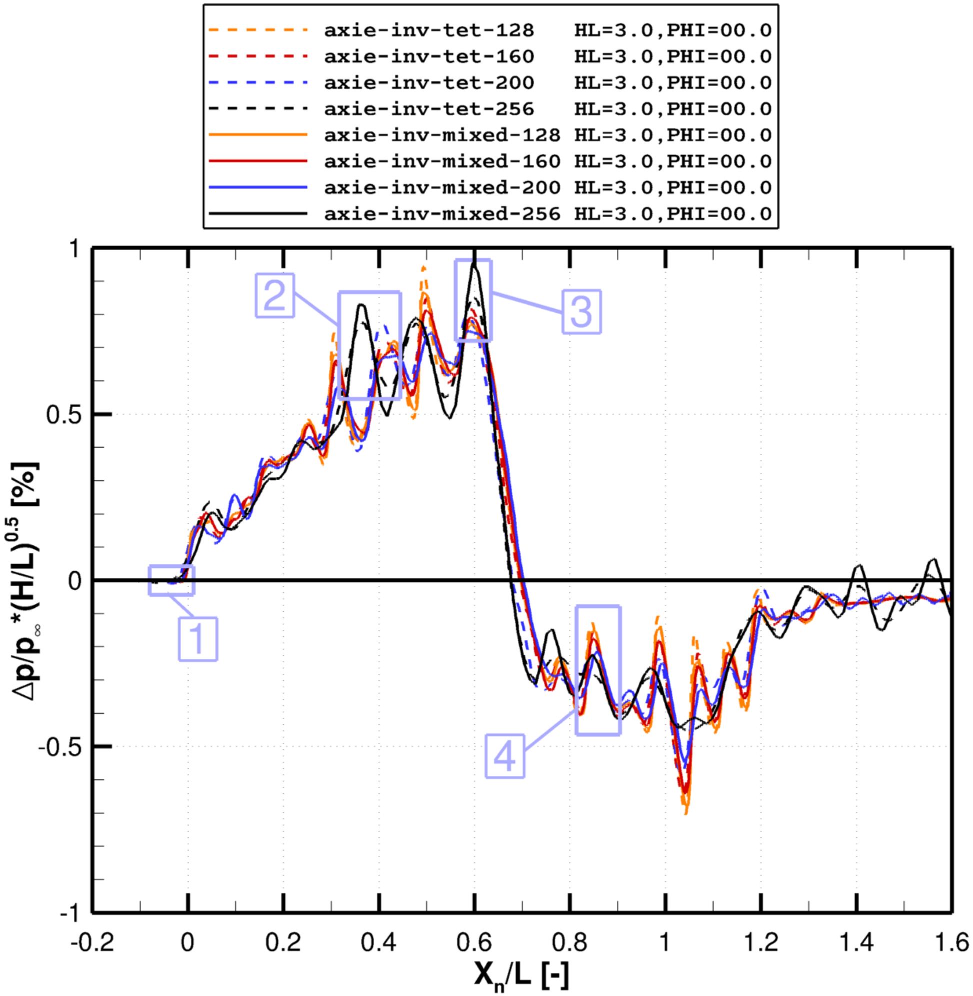

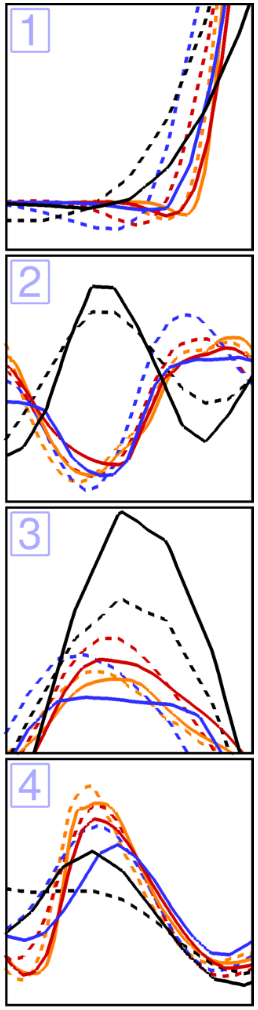

Results AXIE

Signatures H/L=3 (new FF)

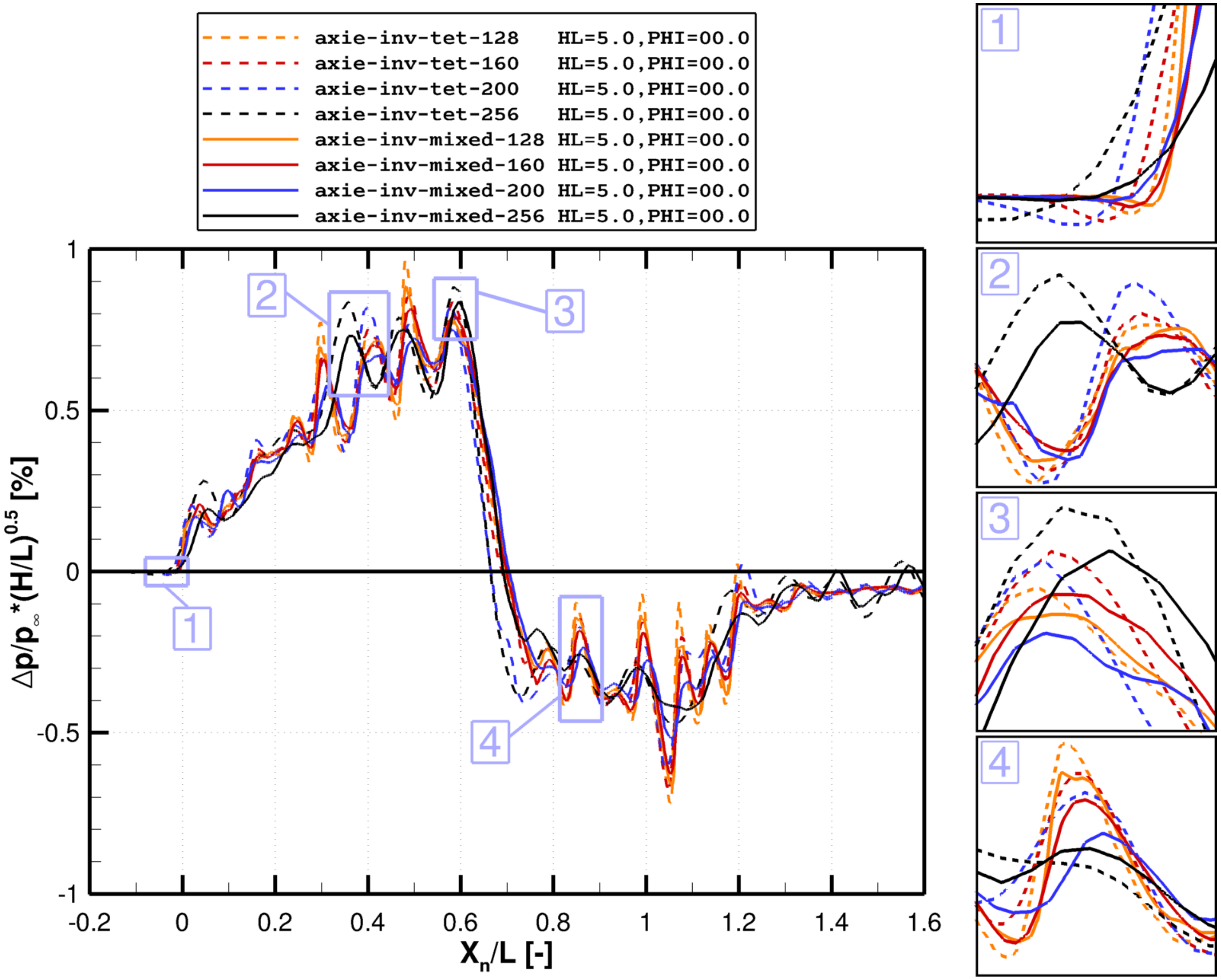

Mesh Induced Shocks and Expansions

axie_R0101_axie-inv-mixed-256

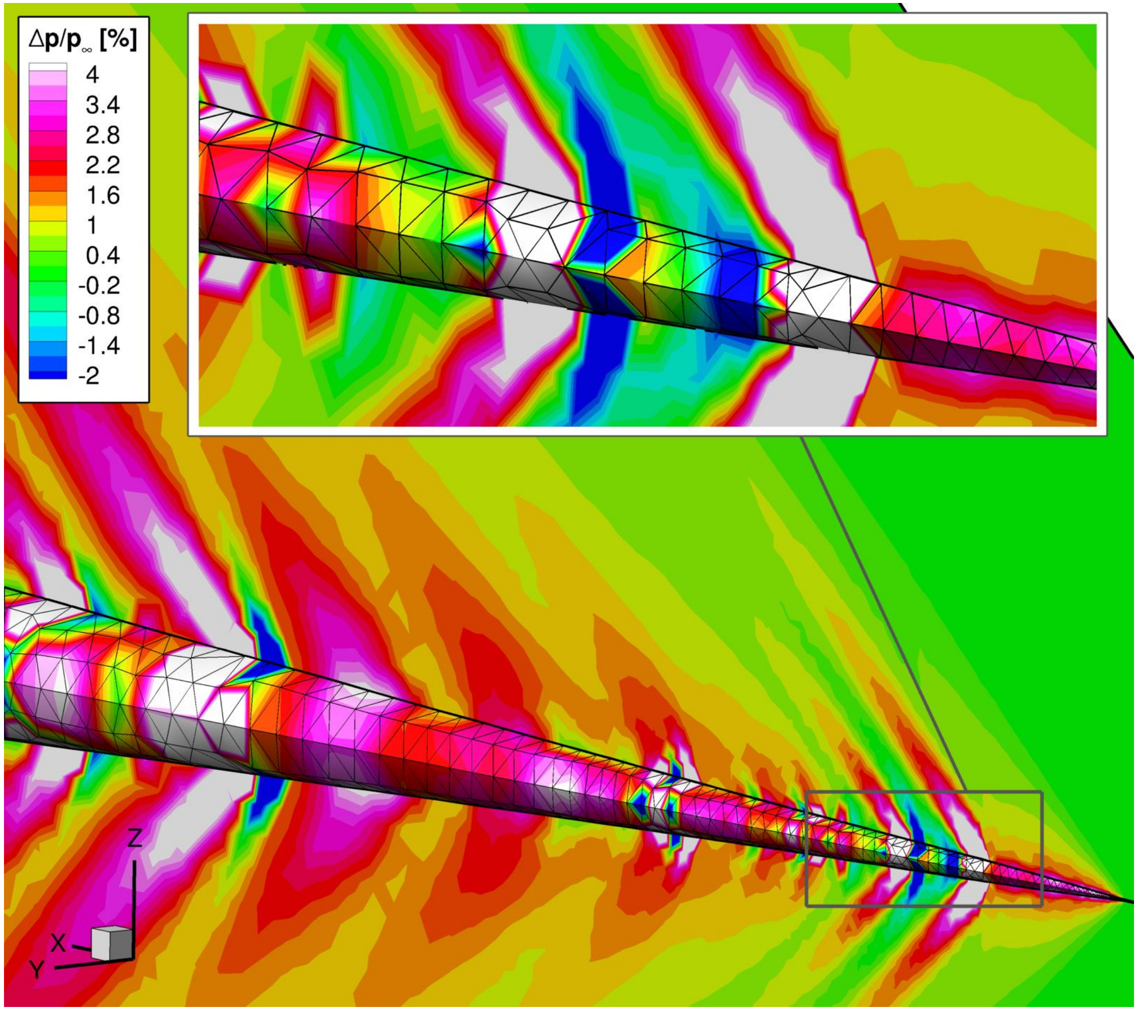

Results JWB

Pressure Contours and near field signatures

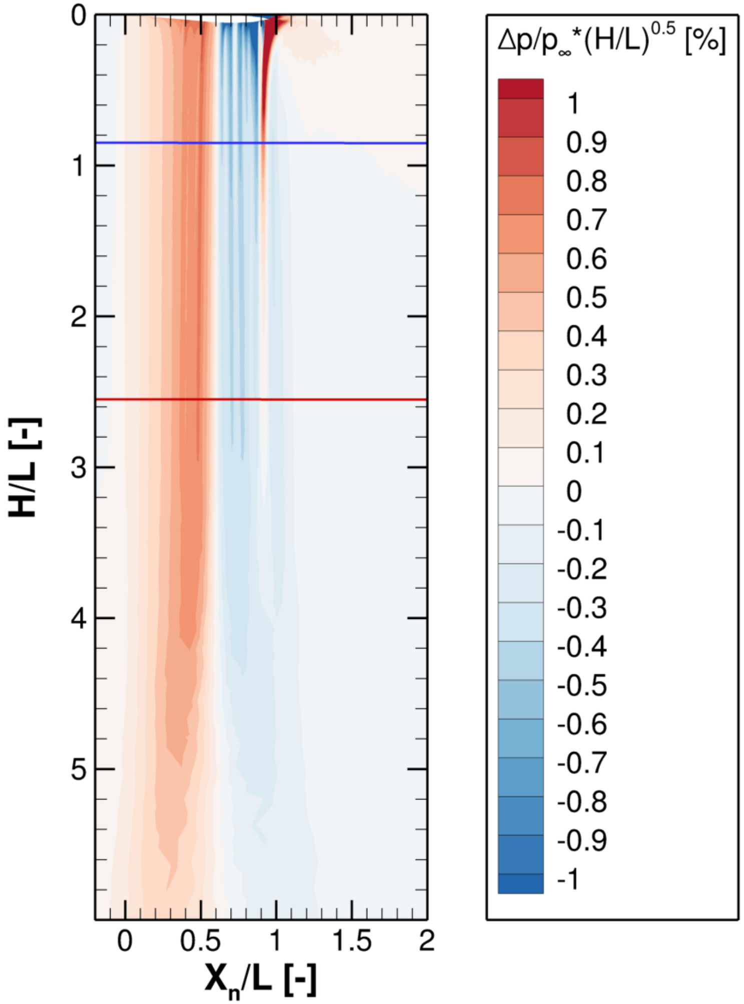

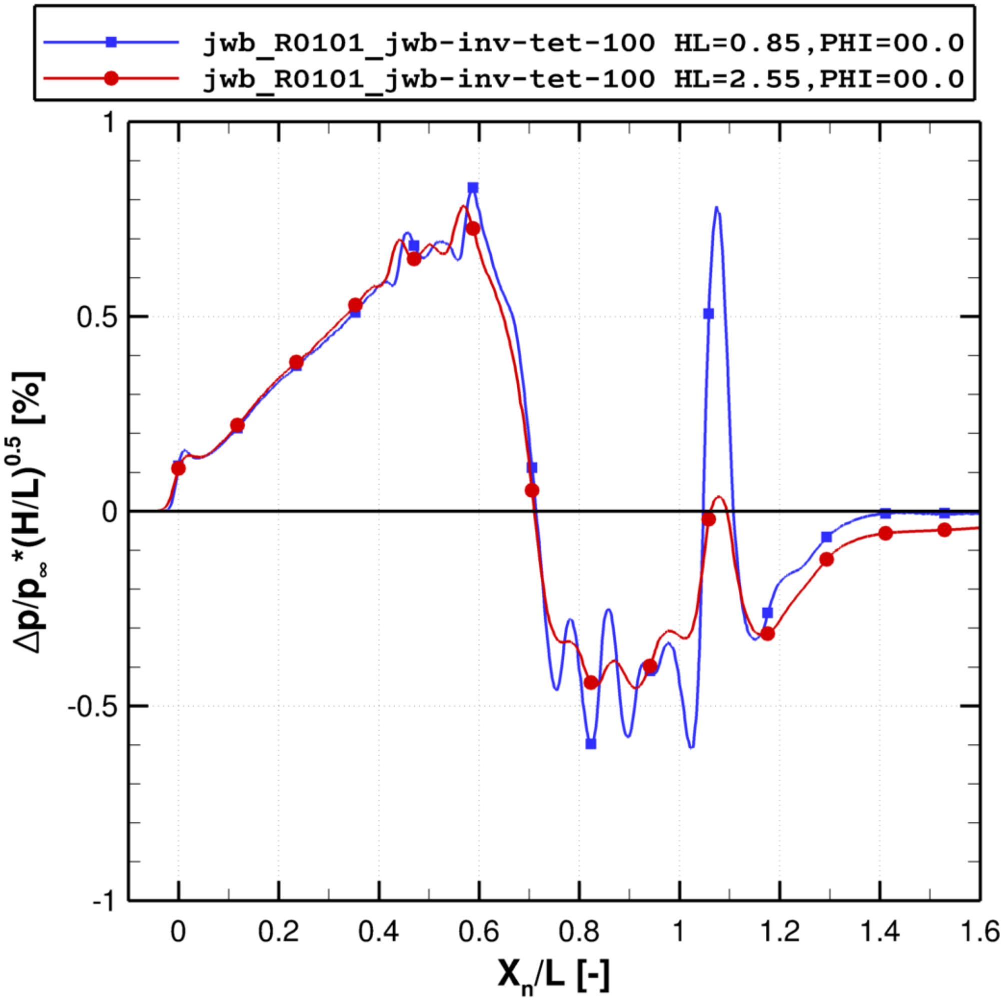

Results JWB

Signature Convergence

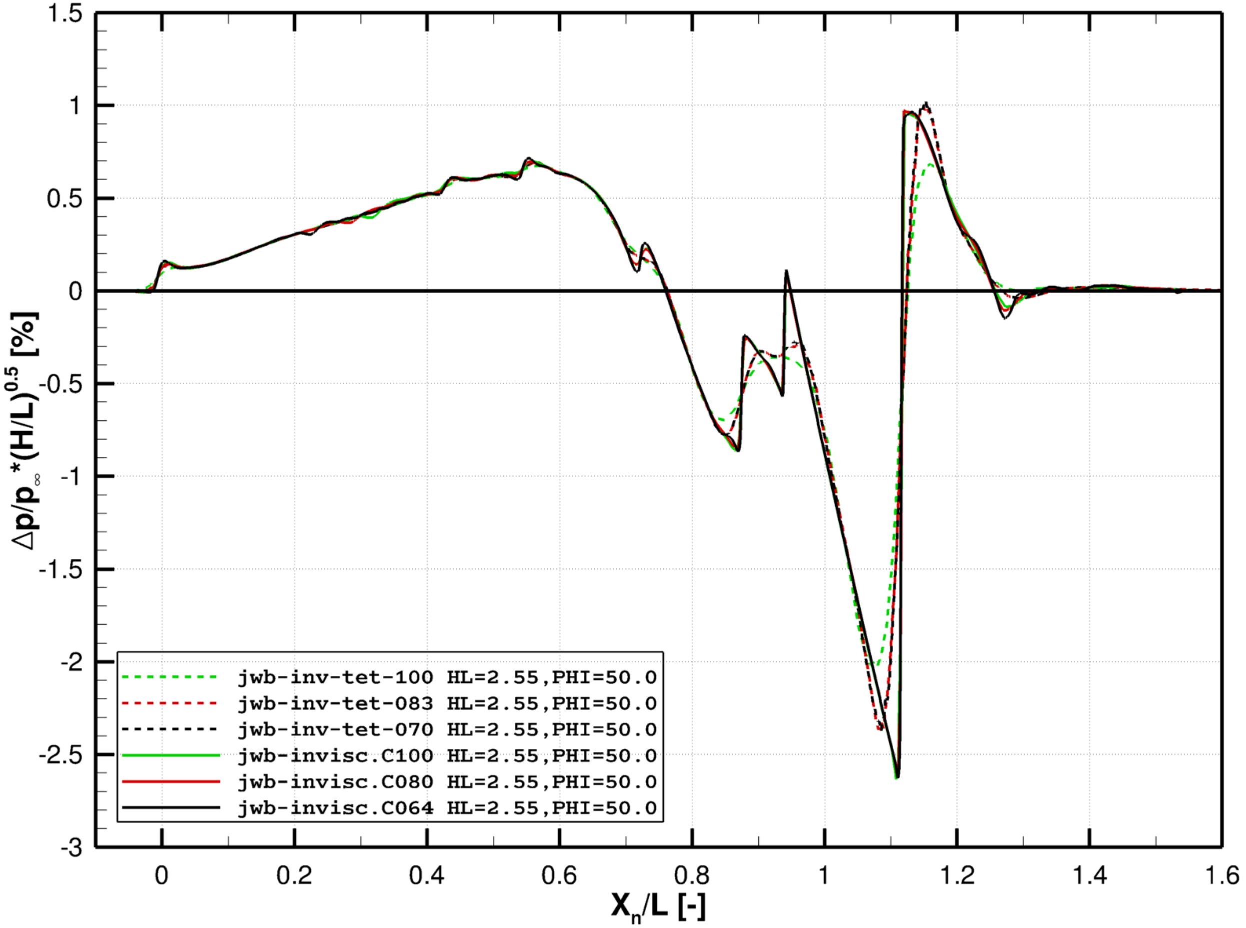

Results C25D flow-through

Pressure Contours and near field signatures

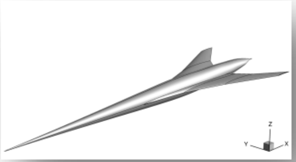

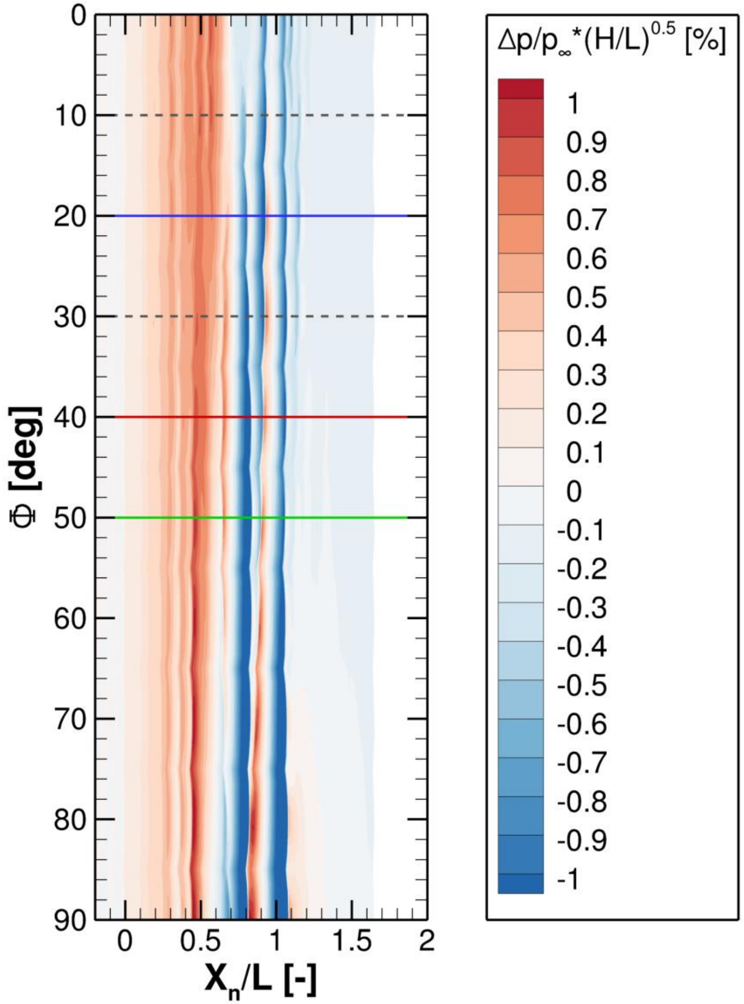

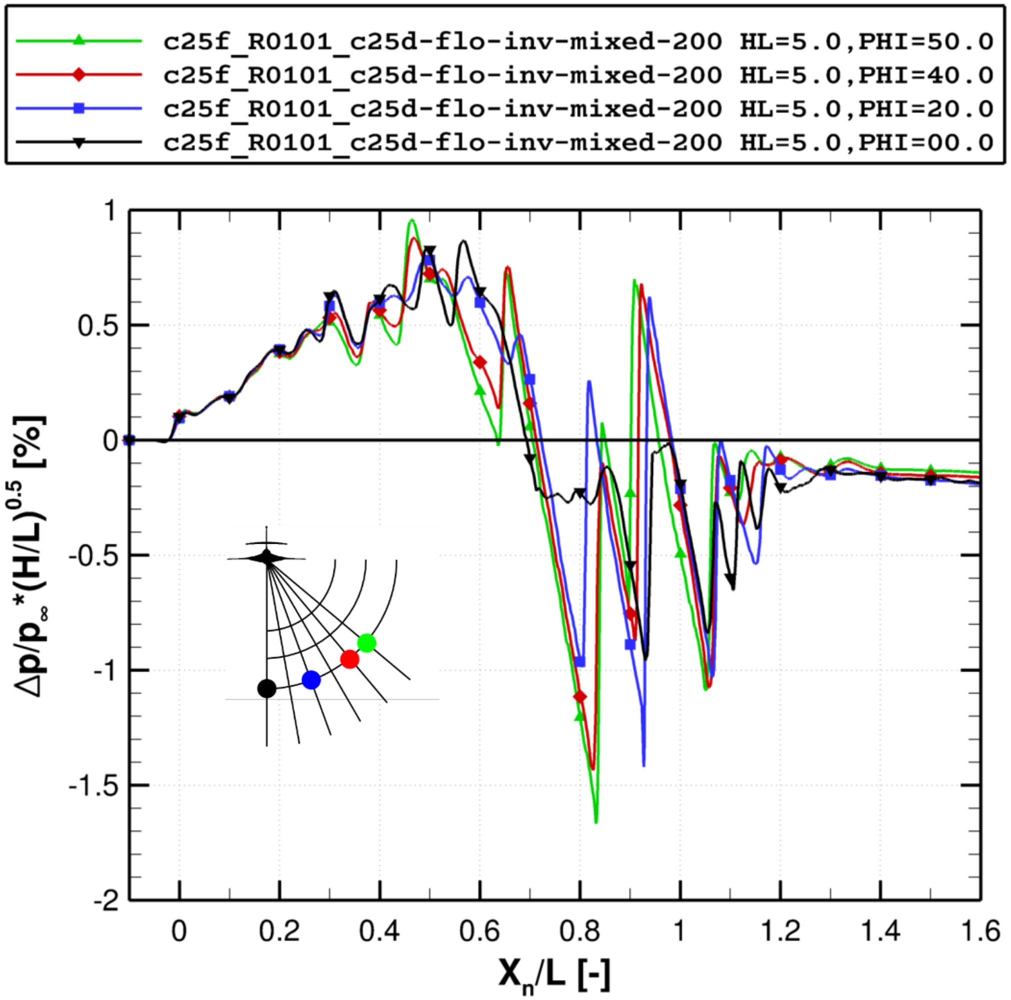

Results C25D flow-through

Signature Convergence

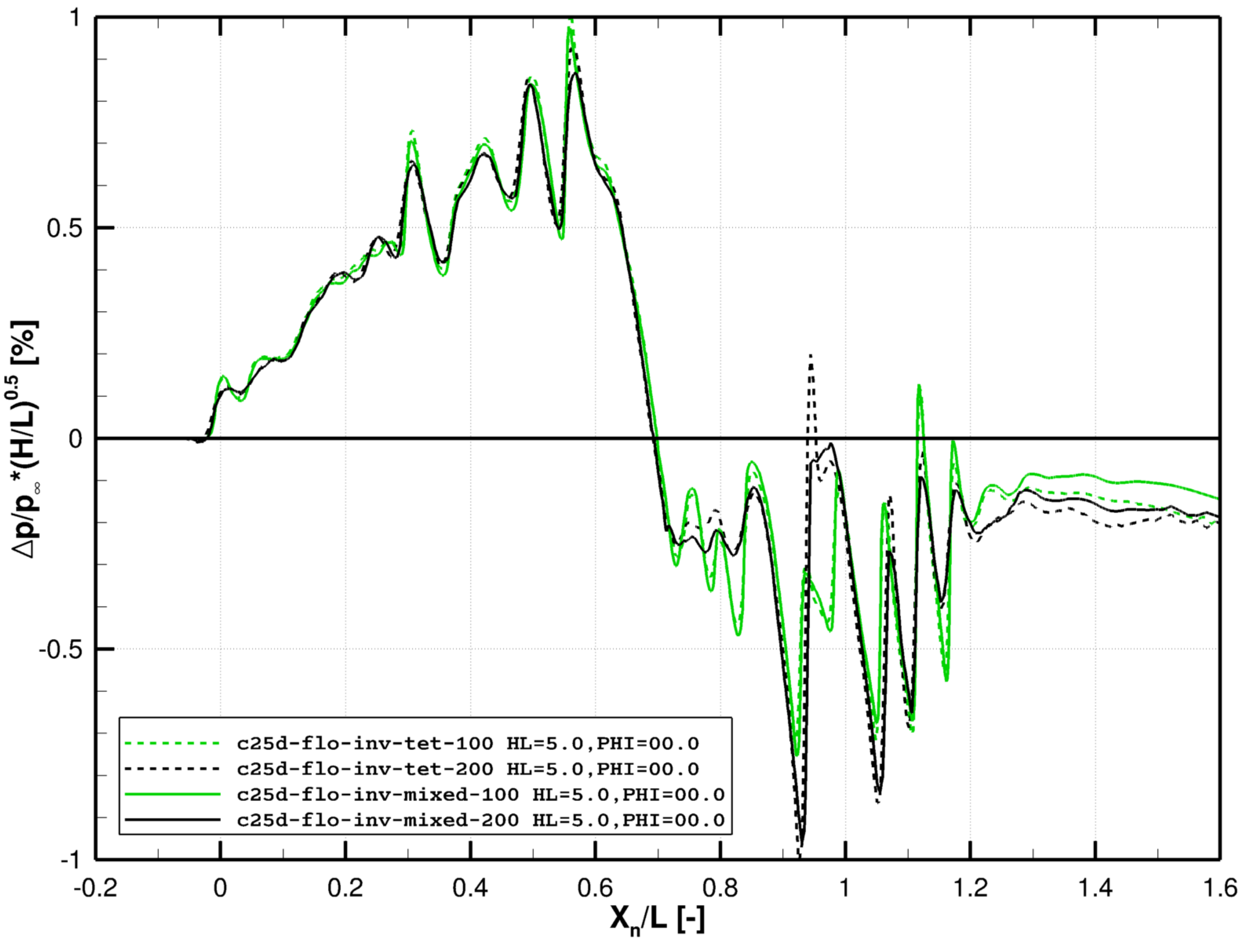

Highlights

Inflow and Farfield Boundary Condition Changes

- Supersonic inflow/outflow
  - Compute boundary fluxes with approximate Riemann solver instead of setting conservative variables at the boundary
  - The gradients of all variables are set to zero in the direction normal to the boundary

- Farfield
  - The farfield fluxes are evaluated via a characteristic method that is in line with the interior face-flux computation.
  - The corresponding flux parameters are inherited from the central, matrix-dissipative scheme

- Convergence improved as side effect (more robust start, significantly less iterations needed and residual lowered by 1-2 orders of magnitude)

Highlights

Unphysical pressures for large H/L at inflow, outflow and farfield boundary conditions

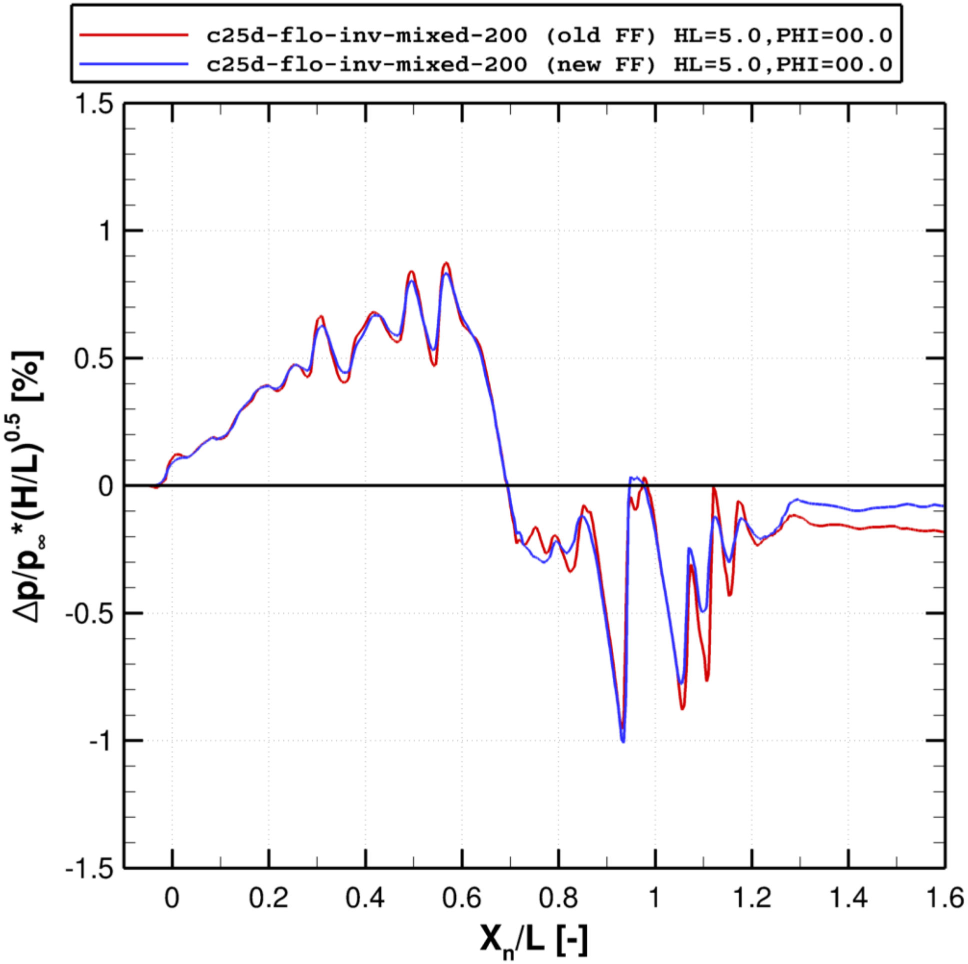

Highlights

Unphysical pressures for large H/L at inflow, outflow and farfield boundary conditions

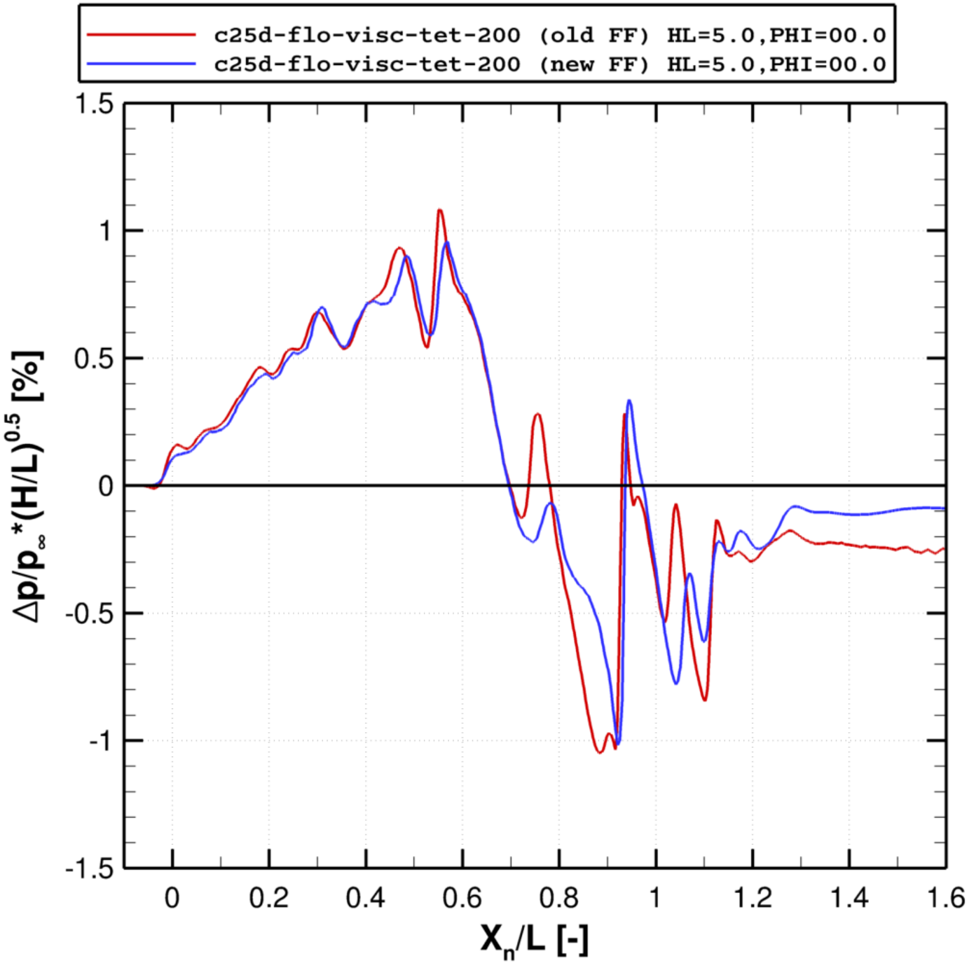

DLR